TeKCEM

Presentation of the MIMOmatch-E patent portfolio

30 September 2019 — version 5

SUMMARY OF THE MIMOmatch-E PATENT PORTFOLIO

Sector: wireless communication
Technical area: antenna tuning, MIMO radio transmission

Table I. Patent families of the MIMOmatch-E patent portfolio	
Title of the patent family	Family
Method for automatically adjusting tunable passive antennas, and automatically tunable antenna array using this method	P63
Method for automatic adjustment of tunable passive antennas and a tuning unit, and apparatus for radio communication using this method	P69
Method for automatically adjusting tunable passive antennas and a tuning unit, and apparatus for radio communication using this method	P70

Status: each patent family includes a granted patent of the U.S.A. Link to the patents

Short description: The MIMOmatch-E portfolio consists of the inventions P63, P69 and P70 of Tekcem, which belong to the space "adaptive antenna tuning for a wireless device using several antennas simultaneously in the same frequency band". All inventions of this portfolio have the following characteristics:

- they use a plurality of tunable passive antennas and are suitable for user equipments (UEs) using MIMO transmission;
- they provide a fast automatic tuning over a broad frequency range, in a manner that complies with the requirements of standards typically applicable to MIMO wireless networks;
- they adaptively compensate the antenna interaction and the effects of the electromagnetic characteristics of the surroundings (including the user interaction), to deliver an optimal automatic tuning, even when antenna tuner losses are significant.

Disclaimer: information contained herein is believed to be reliable, but no warranty is given as to its accuracy or completeness.

MAILING ADDRESS: Tekcem - 12, chemin des Hauts de Clairefontaine - 78580 MAULE - FRANCE
Tel. : 01 34 75 13 65 Int. Tel. : +33 1 34 75 13 65 Web site: http://www.tekcem.com e-mail : info@tekcem.com
TEKCEM : SAS à capital variable / R.C.S. Versailles 512 918 764 / Siret 512 918 764 00014 / APE 7490B

Table of contents

1. Listing of the MIMOmatch-E portfolio

Table II. Items of the MIMOmatch-E patent portfolio						
Item ID	Jurisdiction	Appl. no.	Filing date	Patent or PCT publ. no.	Issue date	Family
P63-A	France	15/02633	17 Dec. 2015	FR1502633	01 Dec. 2017	P63
P63-B	PCT	PCT/IB2016/051400	11 Mar. 2016	WO 2017/103687	N/A	
P63-C	U.S.A.	15/342,663	03 Nov. 2016	9,698,484	04 Jul. 2017	
P69-A	France	FR1770169	21 Feb. 2017	pending	pending	P69
P69-B	PCT	PCT/IB2017/054507	25 Jul. 2017	WO 2018/154366	N/A	
P69-C	U.S.A.	15/694,064	01 Sep. 2017	9,929,460	27 Mar. 2018	
P70-A	France	FR1770175	23 Feb. 2017	pending	pending	P70
P70-B	PCT	PCT/IB2017/054531	26 Jul. 2017	WO 2018/154368	N/A	
P70-C	U.S.A.	15/697,005	06 Sep. 2017	9,912,075	06 Mar. 2018	

At the date of this document, Tekcem is the sole owner of and has good and marketable title to the items listed in Table II, which are free and clear of all liens, mortgages, security interests or other encumbrances, and restrictions on transfer. At the date of this document, **except a patent license agreement with Samsung Electronics Co., Ltd concerning only the family P63**, no rights or licenses have been granted under the items listed in Table II.

2. Notes on terminology

Antenna interaction. Antenna interaction between the antennas of a multiport antenna array results in a significantly non-diagonal impedance matrix. It is caused by a narrow spacing between the antennas, and is more pronounced in the lower frequency bands. Antenna interaction may produce a mismatch loss and noise in the downlink, a mismatch loss and cross modulation in the uplink, and antenna correlation.

Antenna tuner (AT). Traditional antenna tuners have a single input port and a single output port. The inventions P63, P69 and P70 use a multiple-input-port and multiple-output-port antenna tuner, referred to as “multiple-input-port and multiple-output-port tuning unit”. Each patent application includes a detailed definition of a multiple-input-port and multiple-output-port tuning unit. A multiple-input-port and multiple-output-port antenna tuner may consist of several independent single-input-port and single-output-port antenna tuners, but this is not necessary.

Aperture tuning. Aperture tuning means adjusting one or more tunable passive antennas.

Closed-loop. “closed-loop control”, also referred to as “feedback control”, means control in which the control action is made to depend on a measurement of the controlled variable (see “IEC multilingual dictionary of electricity” edited by the *Bureau Central de la Commission Electrotechnique Internationale*).

Effects of the electromagnetic characteristics of the surroundings (EECS). The effects, on a wireless link, of the interaction between the one or more antennas of a user equipment (UE) and the medium surrounding these antennas. These effects comprise:

- ◆ a variation in the impedance of the antenna, or in the impedance matrix of the antennas;
- ◆ a variation in the radiation efficiency;
- ◆ a variation in the directivity of the system formed by the UE and the user.

For instance, the electromagnetic interaction between an antenna and a user holding the UE, often referred to as “user interaction” and illustrated below, can severely degrade the radio link.

Impedance tuning. Impedance tuning means adjusting one or more antenna tuners.

Open-loop. In the literature on antenna tuners, “open-loop” often erroneously refers to a control scheme without measurement of an electrical variable, so that the antenna tuner is typically adjusted only as a function of the operating frequency. In this document and in line with standard terminology, “open-loop control” means control which does not utilize a measurement of the controlled variable (see “IEC multilingual dictionary of electricity” edited by the *Bureau Central de la Commission Electrotechnique Internationale*). This correct definition is also included in the items P69-B, P69-C, P70-B and P70-C.

Tunable passive antenna (TPA). The inventions P63, P69 and P70 use several tunable passive antennas. Each patent application includes a detailed definition of a tunable passive antenna.

User interaction. See Effects of the electromagnetic characteristics of the surroundings (EECS), above.

3. Context and state of the art

In current premium tier mobile phone designs, automatic antenna tuning, which adjusts a tunable passive antenna (TPA) and/or an antenna tuner (AT) to improve performance, has become increasingly prominent as a method to support the growing range of LTE frequencies, and to mitigate possible effects of the electromagnetic characteristics of the surroundings (EECS). For instance, the electromagnetic interaction between an antenna and a user holding the mobile phone, often referred to as *user interaction*, can severely degrade the radio link, unless antenna tuning is implemented.

Antenna tuning is taken into account in MIPI alliance specifications, and many manufacturers provide components for antenna tuning or implement them in LTE user equipments (UEs). For instance, one of the key aspects of the latest high-performance modems of Qualcomm is their antenna tuning capability, which may use “Qualcomm® TruSignal™ antenna boost technology” and “Qualcomm® RF360 dynamic antenna matching tuner”. For instance, an IHS Markit teardown of a Galaxy S8+ found that the smartphone uses both impedance tuning and aperture tuning solutions from Qualcomm, the QAT3550 and the QAT3514.

Antenna tuning can be used to: reduce the size of the antennas, allow to use them on more frequencies, and improve the characteristics of the radio link. Thus, it increases the overall power efficiency, signal consistency, and achievable data speed. For consumers, automatic antenna tuning can provide a better data and voice experience indoors and outdoors, and longer battery life. For original equipment manufacturers (OEMs), automatic antenna tuning may help reduce product size (form factor), and time-to-certification, by addressing the risk of redesign iterations caused by insufficient antenna performance. It is recognized that MIMO radio communication and antenna tuning will play a more important role in UEs for 5G.

However, to our best knowledge, no commercially available automatic antenna tuning system mitigates the antenna interaction between antennas used simultaneously, in the same frequency band, for MIMO radio communication (i.e., provides a scattering matrix, or an impedance matrix, which is diagonal, or close to a diagonal matrix). This capability defines the innovation space “adaptive antenna tuning for a wireless device using several antennas simultaneously in the same frequency band”, and is critical for single-user MIMO below 1.6 GHz. This space comprises the inventions P54 to P62 of Tekcem, which have been previously sold to Samsung Electronics Co., Ltd (see § 7.2 below). These inventions provide solutions to some challenges of single-user MIMO. However, these inventions cannot simultaneously:

- accurately operate over a broad frequency range, as allowed by the combined use of tunable passive antennas and of a multiple-input-port and multiple-output-port antenna tuner;
- provide a fast automatic tuning, in a manner that complies with the requirements of standards typically applicable to MIMO wireless networks; and
- adaptively compensate the antenna interaction and the effects of the electromagnetic characteristics of the surroundings (including the user interaction), to deliver an optimal automatic tuning, even when antenna tuner losses are significant.

4. Technical presentation of the inventions

The patent family P63 is about a method for automatically adjusting tunable passive antennas. Thus, it can be compared to the ninth embodiment of our invention P59 (disclosed in PCT/IB2015/051644 and US patent 9,680,510, assigned to Samsung Electronics Co., Ltd), which has the drawback that several excitations must be applied successively. This characteristic is not compatible with the requirements of all MIMO emission modes of standards typically applicable to MIMO wireless networks. In contrast, according to our invention P63, the excitations can be applied simultaneously, by utilizing the theory presented in § 6.2 and § 6.3 below, which is used in the first, second and third embodiments. As a consequence, the method of P63 is compatible with the requirements of all MIMO emission modes of standards typically applicable to MIMO wireless networks, as pointed out in the PCT application. It is also interesting to compare the patent family P63 to our invention P61 (disclosed in PCT/IB2015/057131 and US appl. No. 15/296,724 allowed on 17 July

2018, assigned to Samsung Electronics Co., Ltd), given that both inventions use closed-loop control to tune an impedance matrix, by delivering tuning control signals to adjustable impedance devices (an "antenna control device" of P63 may be an adjustable impedance device, according to the prior art section of P63).

The patent family P69 is about a method for automatic adjustment of tunable passive antennas and a tuning unit. It combines an automatic adjustment of tunable passive antennas, with an automatic adjustment of a multiple-input-port and multiple-output-port antenna tuner, to simultaneously obtain: an accurate tuning over a broad frequency range, and a fast automatic tuning thanks to the use of open-loop control for the antenna tuner and for the tunable passive antennas.

The patent family P70 is about a method for automatically adjusting tunable passive antennas and a tuning unit. Like the invention P69, it combines an automatic adjustment of tunable passive antennas, with an automatic adjustment of a multiple-input-port and multiple-output-port antenna tuner, to simultaneously obtain: an accurate tuning over a broad frequency range, and a fast automatic tuning thanks to the use of open-loop control for the antenna tuner. Unlike P69, it uses closed-loop control for the tunable passive antennas.

The patent references cited during the prosecution of P63-C, P69-C and P70-C by the USPTO are summarized in Annex A below. Some characteristics of the inventions are summarized in Table III, where a number in brackets, for instance (2), refers to one of the notes following the table, where the column “AT control scheme” refers to the control scheme used to automatically adjust the antenna tuner, and where the column “TPA control scheme” refers to the control scheme used to automatically adjust tunable passive antennas.

Table III. Characteristics of the inventions of the MIMOmatch-E patent portfolio

Family	Antennas	Measurements	AT control scheme	TPA control scheme
P63	multiple	vector at user ports	closed-loop (1)	closed-loop
P69	multiple	vector at output ports	open-loop (2)	open-loop (3)
P70	multiple	vector at output ports	open-loop (2)	closed-loop (4)

Note 1: in P63, the antenna tuner is optional, and always used with closed-loop control (for instance, in the PCT application of P63, see the ninth embodiment starting at page 28, the thirteenth embodiment starting at page 35, and Fig. 9 to Fig. 12).

Note 2: of course, we use the correct meaning of open-loop control (see § 2 above), and the open-loop control scheme of the antenna tuner is based on the measurements at the output ports, so that it provides an accurate automatic tuning, even when antenna tuner losses are significant.

Note 3: for instance, in the PCT application of P69, see page 10 lines 1 to 5; page 12 lines 6 to 8; page 29 lines 19 to 22; page 32 lines 22 to 25; page 41 lines 27 to 31; page 45 lines 4 to 8; claim 2; and claim 11.

Note 4: for instance, in the PCT application of P70, see page 10 lines 1 to 8; page 29 lines 21 to 27; claim 1; and claim 9.

Thus, the inventions of the MIMOmatch-E porfolio can simultaneously:

- accurately operate over a broad frequency range, as allowed by the combined use of tunable passive antennas and of a multiple-input-port and multiple-output-port antenna tuner;
- provide a fast automatic tuning, in a manner that complies with the requirements of standards typically applicable to MIMO wireless networks; and
- adaptively compensate the antenna interaction and the effects of the electromagnetic characteristics of the surroundings (including the user interaction), to deliver an optimal automatic tuning, even when antenna tuner losses are significant.

5. Frequently asked questions

Question 1. Is there any standard-essential patent in the MIMOmatch-E portfolio ?

Answer 1. We do not think so. Note that Tekcem is not a member of any standard-setting organization, and that no patent of the MIMOmatch-E portfolio is subject to FRAND conditions.

Question 2. What is the MIMOmatch-E portfolio useful for ?

Answer 2. The MIMOmatch-E portfolio is very important for manufacturers of UEs, (for instance Samsung, Apple, Huawei, etc), and for the manufacturers of baseband processors (for instance Samsung, Qualcomm, MediaTek, Intel, etc). The rationale is as follows.

It is recognized that, for a premium UE, MIMO transmission and tunable antennas play a role in LTE, and will play a more important role in 5G New Radio. To achieve a good single-user MIMO performance in a real environment, it is necessary to adaptively compensate the antenna interaction and the effects of the electromagnetic characteristics of the surroundings (including the user interaction). We believe that, in our inventions P54 to P63, P69 and P70, we have patented all possible realistic schemes that provide this fundamental attribute. Our inventions P54 to P62 have been sold to Samsung (see § 7.2 below). The remaining key patents in this area are P63, P69 and P70 of the MIMOmatch-E portfolio.

It is not easy to see why P54 to P63, P69 and P70 include all possible realistic schemes providing said fundamental attribute. Please do not hesitate to contact us to discuss this. Note that an analysis of the citations listed in Annex A below shows that we have indeed been the first inventors to address the space “adaptive antenna tuning for a portable wireless device using several antennas simultaneously in the same frequency band”.

Question 3. How does the MIMOmatch-E portfolio compare to the inventions P54 to P62 sold to Samsung ?

Answer 3. It offers many advantages. The best antenna tuning strategies for MIMO wireless transmission use a plurality of tunable passive antennas (TPA) for a coarse tuning, and an antenna tuner (AT) for the fine tuning. This allows an accurate automatic tuning over a broad frequency range. The invention P63 of the MIMOmatch-E portfolio (for which a license was granted to Samsung, see § 1 above) discloses an automatic tuning of TPAs based on measurements during emission, in a manner that is compatible with the requirements of standards typically applicable to MIMO wireless networks. The patents of the MIMOmatch-E portfolio also disclose an automatic tuning of TPAs combined with a fast automatic tuning of an AT, in a manner that is compatible with the requirements of standards typically applicable to MIMO wireless networks. Thus, the inventions of the MIMOmatch-E porfolio are necessary to simultaneously:

- accurately operate over a broad frequency range, as allowed by the combined use of tunable passive antennas and of a multiple-input-port and multiple-output-port antenna tuner;
- provide a fast automatic tuning, in a manner that complies with the requirements of standards typically applicable to MIMO wireless networks; and
- adaptively compensate the antenna interaction and the effects of the electromagnetic characteristics of the surroundings (including the user interaction), to deliver an optimal automatic tuning, even when antenna tuner losses are significant.

These are very important advantages of the MIMOmatch-E portfolio, compared to our inventions sold to Samsung, based on measurements during emission and compatible with MIMO in LTE and 5G (which only use an automatic tuning of an AT). In a nutshell, the inventions of the MIMOmatch-E portfolio are necessary to obtain the best performance.

Question 4. Is any third party currently using an invention of the MIMOmatch-E portfolio ?

Answer 4. We do not think so. This is why, in the middle of § 3 above, we wrote: "however, to our best knowledge, no commercially available automatic antenna tuning system mitigates the interaction between antennas used simultaneously, in the same frequency band, for MIMO radio communication". But we might be wrong. For instance, the advertising about "Qualcomm® TruSignal™ antenna boost technology" and "Qualcomm® RF360 dynamic antenna matching tuner" clearly suggests a UE with an antenna tuning capability for multiple antennas, presumably used for single-user MIMO radio communication. We believe that these products do not currently mitigate the interaction between antennas used simultaneously in the same frequency band. In the opposite case, they might be infringing the MIMOmatch-E portfolio, or one or more of our inventions P54 to P62 purchased by Samsung.

The lack of evidence of use is not the best configuration for an NPE seeking quick profit. This portfolio is meant for a manufacturer who is looking for the best solution for his future products.

Question 5. When are the inventions of the MIMOmatch-E portfolio going to be needed ?

Answer 5. Very soon. Mobile phones with full MIMO capabilities is a quickly emerging market. The 3GPP technical specification ETSI TS 136 306 V15.1.0 (2018-07) defines the current UE categories for LTE. In table 4.1-1 (page 21) of this ETSI document, all categories except UE Category 1 (that is Category 2 to Category 12) include the use of 2 or 4 antennas simultaneously in the DL, since an antenna is required for each layer. In 5G/NR release 15, any UE operating below 6 GHz is required to be able to use multiple antennas simultaneously in the DL (2 or 4 antennas, according to the band), see § 7.2 of the 3GPP technical specification ETSI TS 138 101-1 V15.2.0 (2018-07). In addition, § 6.2D of the same specification provides requirements for the use of multiple antennas simultaneously in the UL. In ETSI TS 138 306 V15.2.0 (2018-09), the maximum numbers of layers (hence, of antennas) supported by a 5G UE in the DL and in the UL are still "to be determined" (see § 4.2.7 of the specification). We see that 5G UEs are going to use multiple antennas simultaneously more aggressively in the DL and in the UL than 4G UEs, in which single-user MIMO is optional. A UE providing real 5G/NR capabilities will need to be able to effectively use several antennas for single-user MIMO over many bands, so that a solution belonging to the space "adaptive antenna tuning for a wireless device using several antennas simultaneously in the same frequency band" will be required. Several manufacturers have begun to design the first 5G phones, which are expected in 2019/2020.

Question 6. Is an infringement of the MIMOmatch-E portfolio easy to detect ?

Answer 6. Yes, for a manufacturer of UE, this is easy.

When the first 5G handsets are available, information about their design will transpire and be useful to detect infringements. Also, it is going to be relatively easy to determine which method is used to perform "adaptive antenna tuning for a wireless device using several antennas simultaneously in the same frequency band", that is: a stupid automatic tuning method using no measurement, or a method that we have sold to Samsung, or the MIMOmatch-E.

Detecting an infringement is easy because you do not need to know the exact algorithms that are being used. To determine the method which is implemented, you can look at the hardware and find out: (a) if TPAs are used; (b) if an AT is used; (c) how the tuning control signals received by the TPAs and/or AT behave when the operating frequency changes; (d) how the tuning control signals received by the TPAs and/or AT behave when an object is moved in the vicinity of the antennas; and (e) if the hardware makes measurements before the antenna tuner or after the antenna tuner. Detecting an infringement only requires an inspection of the UE circuits, and simple measurements across discrete devices. There is no need to look at the silicon inside chips, or to know the signal processing code. All this is simple for a manufacturing company.

6. Some technical details

6.1 About antenna tuner control schemes

In the seventh embodiment of P69, at page 34 of the PCT application, and in the seventh embodiment of P70, at page 34 of the PCT application, it is explained that:
— the process "delivering tuning control signals to the tuning unit" uses an algorithm to determine the one or more tuning unit adjustment instructions;
— the algorithm uses the selected frequency and the q real quantities depending on an impedance matrix seen by the output ports, which are representative of an impedance matrix seen by the output ports at the end of the process "delivering antenna control signals to the tunable passive antennas"; and
— a possible algorithm may for instance use the iterative computation technique presented in Section 4 of an article shown in Annex B below, this possible algorithm being accurate, because it takes the losses in the multiple-input-port and multiple-output-port tuning unit into account.

Section 8 of the article shown in Annex B below is also important, because is proves that an accurate open-loop control of a multiple-input-port and multiple-output-port antenna tuner is feasible. Some questions raised by this article are treated in a more recent article, shown in Annex C below.

6.2 A first theorem

The following theorem is used in the first embodiment of P63, at page 12 of the PCT application. Let E be any suitable subspace of the set of complex functions of one real variable, regarded as a vector space over the field of complex numbers. Let us number the user ports from 1 to m, and let us number the excitations from 1 to m, in such a way that, if we use t to denote time, for any $a \in \{1,..., m\}$, the excitation number a consists of a current $i_a(t)$ applied to the user port number a, which is a bandpass signal of carrier frequency f_C and of complex envelope $i_{E\,a}(t)$, the complex envelopes $i_{E\,1}(t),..., i_{E\,m}(t)$ being linearly independent in E. Let us use $\mathbf{i}_E(t)$ to denote the column vector of the complex envelopes $i_{E\,1}(t),..., i_{E\,m}(t)$. For any $a \in \{1,..., m\}$, let us use $u_a(t)$ to denote the voltage across the user port number a. We assert that $u_a(t)$ is a bandpass signal of carrier frequency f_C. Let us use $u_{E\,a}(t)$ to denote the complex envelope of $u_a(t)$. Using $\mathbf{u}_E(t)$ to denote the column vector of the complex envelopes $u_{E\,1}(t),..., u_{E\,m}(t)$, we maintain that, if the bandwidth of the complex envelopes $i_{E\,1}(t),..., i_{E\,m}(t)$ is sufficiently narrow, we have

$$\mathbf{u}_E(t) = \mathbf{Z}_U\ \mathbf{i}_E(t) \tag{1}$$

where the impedance matrix $\mathbf{Z}_U$ is considered at the carrier frequency.

The proof of this theorem is the following. For any $a \in \{1,..., m\}$, let $I_a(f)$ be the Fourier transform of $i_a(t)$ and let $U_a(f)$ be the Fourier transform of $u_a(t)$. Let $\mathbf{I}(f)$ be the column vector of $I_1(f),..., I_m(f)$. Let $\mathbf{U}(f)$ be the column vector of $U_1(f),..., U_m(f)$. Since we are considering a passive linear time invariant (LTI) circuit, we can say that at any frequency f, we have

$$\mathbf{U}(f) = \mathbf{Z}_U(f)\,\mathbf{I}(f) \tag{2}$$

so that, for any $a \in \{1,..., m\}$, $u_a(t)$ is a bandpass signal of carrier frequency f_C.

For any $a \in \{1,..., m\}$, let $I_{E\,a}(f)$ be the Fourier transform of $i_{E\,a}(t)$ and let $U_{E\,a}(f)$ be the Fourier transform of $u_{E\,a}(t)$. Let $\mathbf{I}_E(f)$ be the column vector of $I_{E\,1}(f),..., I_{E\,m}(f)$. Let $\mathbf{U}_E(f)$ be the column vector of $U_{E\,1}(f),..., U_{E\,m}(f)$. Using W to denote the bandwidth of the excitations, which is also the bandwidth of the complex envelopes $i_{E\,1}(t),..., i_{E\,m}(t)$, we find that:
— at any frequency outside the frequency interval $[-W/2, W/2]$, $\mathbf{I}_E(f)$ is a null vector and $\mathbf{U}_E(f)$ is a null vector;
— at any frequency in the frequency interval $[-W/2, W/2]$, we have

$$\mathbf{U}_E(f) = \mathbf{Z}_U(f + f_C)\,\mathbf{I}_E(f) \tag{3}$$

If the bandwidth of the complex envelopes $i_{E\,1}(t),\ldots, i_{E\,m}(t)$ is sufficiently narrow, we can write

$$\mathbf{U}_E(f) \approx \mathbf{Z}_U(f_C)\,\mathbf{I}_E(f) \tag{4}$$

Taking an inverse Fourier transform, we obtain

$$\mathbf{u}_E(t) \approx \mathbf{Z}_U(f_C)\,\mathbf{i}_E(t) \tag{5}$$

which is the wanted result. We have proved the first theorem.

6.3 A second theorem

The following theorem is used in the third embodiment of P63, at page 19 of the PCT application, in the fifth embodiment of P69, at page 26 of the PCT application, and in the fifth embodiment of P70, at page 26 of the PCT application. A weaker form of the theorem (with zero secondary components) is used in the second embodiment of P63, at page 17 of the PCT application, in the fourth embodiment of P69, at page 24 of the PCT application, and in the fourth embodiment of P70, at page 24 of the PCT application. Let E be any subspace of the set of complex functions of one real variable, regarded as a vector space over the field of complex numbers. Let us use $<f|\, g>$ to denote a scalar product of two functions $f \in E$ and $g \in E$, which may be any scalar product satisfying the properties of conjugate symmetry, linearity in the second argument, and positivity (we do not require positive definiteness).

Let us assume that, for any $a \in \{1,\ldots, m\}$, the complex envelope $i_{E\,a}(t)$ is of the form

$$i_{E\,a}(t) = i_{C\,a}(t) + i_{D\,a}(t) \tag{6}$$

where $i_{C\,a}(t) \in E$ is the primary component of the complex envelope, and $i_{D\,a}(t) \in E$ is the secondary component of the complex envelope, the primary components $i_{C\,1}(t),\ldots, i_{C\,m}(t)$ of the m complex envelopes being orthogonal to each other, and each of the primary components $i_{C\,1}(t),\ldots, i_{C\,m}(t)$ of the m complex envelopes being orthogonal to each of the secondary components $i_{D\,1}(t),\ldots, i_{D\,m}(t)$ of the m complex envelopes. If the scalar product of any one of the primary components of the m complex envelopes and itself is nonzero, then:

- the m complex envelopes $i_{E\,1}(t),\ldots, i_{E\,m}(t)$ are linearly independent;
- using S to denote the span of $i_{E\,1}(t),\ldots, i_{E\,m}(t)$ in E, for any $g(t) \in$ S and for any $b \in \{1,\ldots, m\}$, the b-th coordinate of the vector $g(t)$ in the basis $i_{E\,1}(t),\ldots, i_{E\,m}(t)$ of S, denoted by μ_b is given by

$$\mu_b = \frac{\left\langle i_{Cb} \middle| g \right\rangle}{\left\langle i_{Cb} \middle| i_{Cb} \right\rangle} \tag{7}$$

The proof of this theorem is the following. For any complex numbers $\lambda_1,\ldots, \lambda_m$ such that

$$\sum_{a=1}^{m} \lambda_a i_{Ea} = \mathbf{0} \tag{8}$$

we have, for any $b \in \{1,\ldots, m\}$,

$$\left\langle i_{Cb} \middle| \sum_{a=1}^{m} \lambda_a i_{Ea} \right\rangle = \left\langle i_{Cb} \middle| \sum_{a=1}^{m} \lambda_a \left(i_{Cb} + i_{Db} \right) \right\rangle = \lambda_b \left\langle i_{Cb} \middle| i_{Cb} \right\rangle = 0 \tag{9}$$

Since we assume that $< i_{C\,b} \mid i_{C\,b} > \neq 0$, it follows that $\lambda_b = 0$. Thus, $i_{E\,1}(t),\ldots, i_{E\,m}(t)$ are linearly independent. Let now assume that m complex numbers $\mu_1,\ldots, \mu_m$ are such that

$$\sum_{a=1}^{m} \mu_a i_{E\,a} = g \tag{10}$$

we have, for any $b \in \{1,..., m\}$,

$$\left\langle i_{Cb} \middle| g \right\rangle = \left\langle i_{Cb} \middle| \sum_{a=1}^{m} \mu_a \left(i_{Cb} + i_{Db} \right) \right\rangle = \mu_b \left\langle i_{Cb} \middle| i_{Cb} \right\rangle \tag{11}$$

Since we assume that $< i_{C\,b} \mid i_{C\,b} > \neq 0$, (7) is a consequence of (11). We have proved the second theorem.

6.4 A third theorem and its corollary

The following theorem is used in the third embodiment of P69, at the page 21 of the PCT application, and in the third embodiment of P70, at the page 21 of the PCT application. Let E be a subspace of the set of complex functions of one real variable, regarded as a vector space over the field of complex numbers. Let us number the input ports from 1 to m, and number the excitations from 1 to m, in such a way that, if we use t to denote time, for any $a \in \{1,..., m\}$, the excitation number a consists of a current $i_a(t)$ applied to the input port number a, which is a bandpass signal of carrier frequency f_C and of complex envelope $i_{E\,a}(t)$, the complex envelopes $i_{E\,1}(t)$,..., $i_{E\,m}(t)$ lying in E. We assert that, if the bandwidth of the complex envelopes $i_{E\,1}(t)$,..., $i_{E\,m}(t)$ is sufficiently narrow, then, for any $a \in \{1,..., m\}$, any voltage or current measured at anyone of the output ports and caused by the excitation number a is a bandpass signal whose complex envelope is proportional to $i_{E\,a}(t)$, the coefficient of proportionality being complex and time-independent.

The proof of this theorem is the following. For any $a \in \{1,..., m\}$, let $I_a(f)$ be the Fourier transform of $i_a(t)$. Let $\mathbf{I}(f)$ be the column vector of $I_1(f)$,..., $I_m(f)$. Let $u(t)$ be a voltage measured between any two nodes of the circuit and for any $a \in \{1,..., m\}$ let $u_a(t)$ be the voltage measured between these nodes and caused by the excitation number a. Let $U(f)$ be the Fourier transform of $u(t)$ and for any $a \in \{1,..., m\}$, let $U_a(f)$ be the Fourier transform of $u_a(t)$. Let $j(t)$ be a current measured in any branch of the circuit and for any $a \in \{1,..., m\}$ let $j_a(t)$ be the current measured in this branch and caused by the excitation number a. Let $J(f)$ be the Fourier transform of $j(t)$ and for any $a \in \{1,..., m\}$, let $J_a(f)$ be the Fourier transform of $j_a(t)$. Since we are considering a passive LTI circuit, we can say that at any frequency f, there exists a row vector $\mathbf{Z}(f) = (Z_1(f),..., Z_m(f))$ and a row vector $\mathbf{K}(f) = (K_1(f),..., K_m(f))$ such that

$$U(f) = \mathbf{Z}(f)\, \mathbf{I}(f) \tag{12}$$

and

$$I(f) = \mathbf{K}(f)\, \mathbf{I}(f) \tag{13}$$

For any $a \in \{1,..., m\}$, at any frequency f, we consequently have

$$U_a(f) = Z_a(f)\, I_a(f) \tag{14}$$

and

$$J_a(f) = K_a(f)\, I_a(f) \tag{15}$$

so that $u_a(t)$ and $j_a(t)$ are bandpass signals which can be regarded as having the same carrier frequency f_C and the same bandwidth W_a as $i_a(t)$. For any $a \in \{1,..., m\}$, let $u_{E\,a}(t)$ be the complex envelope of $u_a(t)$, and let $j_{E\,a}(t)$ be the complex envelope of $j_a(t)$. For any $a \in \{1,..., m\}$, let $U_{E\,a}(f)$ be the Fourier transform of $u_{E\,a}(t)$ and let $J_{E\,a}(f)$ be the Fourier transform of $j_{E\,a}(t)$. We can say that:
— at any frequency outside the frequency interval $[-W_a/2, W_a/2]$, we have $I_{E\,a}(f) = J_{E\,a}(f) = 0$ A/Hz and $U_{E\,a}(f) = 0$ V/Hz;
— at any frequency in the frequency interval $[-W_a/2, W_a/2]$, we have

$$U_{E\,a}(f) = Z_a(f + f_C)\, I_{E\,a}(f) \tag{16}$$

and

$$J_{E\,a}(f) = K_a(f + f_C)\, I_{E\,a}(f) \tag{17}$$

If the bandwidth of the complex envelopes $i_{E\,a}(t)$ is sufficiently narrow, we can write

$$U_{E\,a}(f) \approx Z_a(f_C)\, I_{E\,a}(f) \tag{18}$$

and

$$J_{E\,a}(f) \approx K_a(f_C)\, I_{E\,a}(f) \tag{19}$$

Taking inverse Fourier transforms, we obtain

$$u_{E\,a}(t) \approx Z_a(f_C)\, i_{E\,a}(t) \tag{20}$$

and

$$j_{E\,a}(t) \approx K_a(f_C)\, i_{E\,a}(t) \tag{21}$$

which completes the proof of the third theorem.

This theorem entails the following corollary. Let us use S to denote the span of $i_{E\,1}(t)$,..., $i_{E\,m}(t)$ in E. We assume that the complex envelopes $i_{E\,1}(t)$,..., $i_{E\,m}(t)$ are linearly independent in E. Thus, $i_{E\,1}(t)$,..., $i_{E\,m}(t)$ is a basis of S. We maintain that any voltage or current measured at anyone of the output ports and caused by the excitations is a bandpass signal of carrier frequency f_C, whose complex envelope lies in S ; and that, for any integer a greater than or equal to 1 and less than or equal to m, the product of the a-th coordinate of the complex envelope of this voltage or current in the basis $i_{E\,1}(t)$,..., $i_{E\,m}(t)$ and the vector $i_{E\,a}(t)$ is equal to the part of the complex envelope of this voltage or current which is caused by the excitation number a.

The proof of this corollary is the following. By (12) and (13), any voltage or current measured at anyone of the output ports and caused by the excitations is a bandpass signal of carrier frequency f_C. Using the same notations as for the theorem and its proof, using $u_E(t)$ to denote the complex envelope of $u(t)$, and $j_E(t)$ to denote the complex envelope of $j(t)$, we can use (20) and (21) and linearity to obtain

$$u_E(t) = \sum_{a=1}^{m} u_{E\,a}(t) \approx \sum_{a=1}^{m} Z_a(f_C)\, i_{E\,a}(t) \tag{22}$$

and

$$j_E(t) = \sum_{a=1}^{m} j_{E\,a}(t) \approx \sum_{a=1}^{m} K_a(f_C)\, i_{E\,a}(t) \tag{23}$$

which show that $Z_1(f_C)$,..., $Z_m(f_C)$ are the coordinates of $u_E(t)$ in the basis $i_{E\,1}(t)$,..., $i_{E\,m}(t)$, and that $K_1(f_C)$,..., $K_m(f_C)$ are the coordinates of $j_E(t)$ in this basis. This completes the proof of the corollary.

7. Presentation of Tekcem

7.1 Business model of Tekcem

The main business of Tekcem has three steps: first, Tekcem purchases R&D work of the Excem group, in the form of reports and software, the report contractually including the description of inventions; second, Tekcem files and prosecutes patent applications for said inventions; third, Tekcem sells intellectual property rights for the inventions (patent applications and patents), and, separately, the know-how and software.

7.2 Information about inventions previously sold by Tekcem

Tekcem has sold the following 13 inventions of the Excem group in the area of radio communication, under the trademark MIMOmatch:

[P62] French patent appl. 15/01780 of 26 August 2015, international appl. PCT/IB2015/057161 of 17 September 2015 (WO 2017/033048), and US patent No. 9,966,930. Method for automatically adjusting a tuning unit, and automatic tuning system using this method. Sold to Samsung Electronics, Co, Ltd in 2016, as a part of patent porfolio MIMOmatch-D.

[P61] French patent appl. 15/01290 of 22 June 2015, international appl. PCT/IB2015/057131 of 16 September 2015 (WO 2016/207705), and US patent No. 10,116,057. Method and apparatus for automatic tuning of an impedance matrix, and radio transmitter using this apparatus. Sold to Samsung Electronics, Co, Ltd in 2016, as a part of patent porfolio MIMOmatch-D.

[P60] French patent appl. 14/01221 of 28 May 2014, international appl. PCT/IB2015/052974 of 23 April 2015 (WO 2015/181653), and US patent No. 10,224,901. Radio communication using a plurality of selected antennas. Sold to Samsung Electronics, Co, Ltd in 2015, as a part of patent porfolio MIMOmatch-C.

[P59] French patent appl. 14/00666 of 20 March 2014, international appl. PCT/IB2015/051644 of 6 March 2015 (WO 2015/140660), and US patent No. 9,680,510. Radio communication using tunable antennas and an antenna tuning apparatus. Sold to Samsung Electronics, Co, Ltd in 2015, as a part of patent porfolio MIMOmatch-C.

[P58] French patent appl. 14/00606 of 13 March 2014, international appl. PCT/IB2015/051548 of 3 March 2015 (WO 2015/136409), and US patent No. 9,654,162. Radio communication using multiple antennas and localization variables. Sold to Samsung Electronics, Co, Ltd in 2015, as a part of patent porfolio MIMOmatch-C.

[P57] French patent appl. 13/00878 of 15 April 2013, international appl. PCT/IB2014/058933 of 12 February 2014 (WO 2014/170766), and US patent No. 9,077,317. Method and apparatus for automatically tuning an impedance matrix, and radio transmitter using this apparatus. Sold to Samsung Electronics, Co, Ltd in 2015, as a part of patent porfolio MIMOmatch-B.

[P56] French patent appl. 13/00665 of 21 March 2013, international appl. PCT/IB2013/060481 of 28 November 2013 (WO 2014/147458), and US patent No. 9,294,174. Method and device for radio reception using a plurality of antennas and a multiple-input-port and multiple-output-port amplifier. Sold to Samsung Electronics, Co, Ltd in 2015, as a part of patent porfolio MIMOmatch-B.

[P55] French patent appl. 12/02564 of 27 September 2012, international appl. PCT/IB2013/058574 of 16 September 2013 (WO 2014/049486), and US patent No. 9,337,534. Method and device for radio reception using an antenna tuning apparatus and a plurality of antennas. Sold to Samsung Electronics, Co, Ltd in 2015, as a part of patent porfolio MIMOmatch-B.

[P54] French patent appl. 12/02542 of 25 September 2012, international appl. PCT/IB2013/058423 of 10 September 2013 (WO 2014/049475), and US patents No. 9,621,132 and No. 10,187,033. Antenna tuning apparatus for a multiport antenna array. Sold to Samsung Electronics, Co, Ltd in 2015, as a part of patent porfolio MIMOmatch-B.

[P41] French patent appl. 08/03982 of 11 July 2008, international appl. PCT/IB2009/051358 of 31 March 2009 (WO 2010/004445), and US patent No. 7,952,429. Multiple-input and multiple-output amplifier having pseudo-differential inputs. Sold to Apple, Inc. in 2012, as a part of patent porfolio MIMOmatch-A.

[P34] French patent appl. 06/06502 of 18 July 2006, international appl. PCT/IB2007/001589 of 5 June 2007 (WO 2008/010035), and US patent No. 7,983,645. Method and device for radio reception using a plurarity of antennas. Sold to Apple, Inc. in 2012, as a part of patent porfolio MIMOmatch-A.

[P33] French patent appl. 06/05633 of 23 June 2006, international appl. PCT/IB2007/001344 of 26 April 2007 (WO 2008/001168), and US patent No. 7,940,119. Multiple-input and multiple-output amplifier using mutual induction in the feedback network. Sold to Apple, Inc. in 2012, as a part of patent porfolio MIMOmatch-A.

[P30] French patent appl. 06/00388 of 17 January 2006, international appl. PCT/IB2006/003950 of 19 December 2006 (WO 2007/083191), and US patent No. 7,642,849. Multiple-input and multiple-output amplifier. Sold to Apple, Inc. in 2012, as a part of patent porfolio MIMOmatch-A.

Thus, Tekcem sold, in the area of radio communication:

- 9 inventions (P54 to P62) to Samsung Electronics, Co, Ltd, in 2015 and 2016; and
- 4 inventions (P30, P33, P34 and P41), to Apple, Inc., in 2012.

Tekcem also sold 16 inventions on signal integrity and integrated circuit interfaces, including 2 inventions sold to Apple, Inc. in 2012.

8. The inventors

The inventors of the MIMOmatch-E portfolio are Evelyne Clavelier and Frédéric Broyde.

Link to an on-line list of their patent applications

Link to an on-line list of their published articles

Evelyne Clavelier was born in France in 1961. She received the M.S. degree in physics engineering from the Ecole Nationale Supérieure d'Ingénieurs Electriciens de Grenoble (ENSIEG). She is a senior member of the IEEE.

She is co-founder of the Excem corporation, based in Maule, France. She is CEO of Excem. She is also manager of Eurexcem (a subsidiary of Excem) and President of Tekcem, a company selling or licensing intellectual property rights. She is also an active engineer and researcher. Her current research area is radio communications. She has also done research work in the areas of electromagnetic compatibility (EMC) and signal integrity. She has taken part in many electronic design and software design projects of Excem.

Prior to starting Excem in 1988, she worked for Schneider Electrics (in Grenoble, France), STMicroelectronics (in Grenoble, France), and Signetics (in Mountain View, USA).

Ms. Clavelier is the author or a co-author of about 80 technical papers. She is co-inventor of about 80 patent families. She is a licensed radio amateur (F1PHQ).

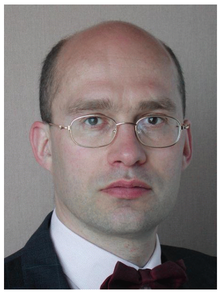

Frédéric Broydé was born in France in 1960. He received the M.S. degree in physics engineering from the Ecole Nationale Supérieure d'Ingénieurs Electriciens de Grenoble (ENSIEG) and the Ph.D. in microwaves and microtechnologies from the Université des Sciences et Technologies de Lille (USTL). He is a senior member of the IEEE.

He co-founded the Excem corporation in May 1988, a company providing engineering and research and development services. He is president and CTO of Excem. Most of his activity is allocated to engineering and research in electronics. Currently, his most active research areas is wireless transmission systems, with an emphasis on antenna tuning.

Dr. Broydé is author or co-author of about 100 technical papers, and inventor or co-inventor of about 80 patent families, for which 48 US patents have been granted. He is a licensed radio amateur (F5OYE).

Annexes

ANNEX A

Patent citations listed in P63-C, P69-C and P70-C

Table 1: cited U.S. applications

	cited in:				
Pub. No.	P63	P69	P70	Status	Applicant
2003/0219035	yes			granted as 7,260,424	Airify Communications, Inc.
2014/0159971	yes			granted as 9,537,223	University of Birmingham
2015/0078485	yes			granted as 9,077,317	Tekcem [P57]
2015/0372656			yes	granted as 9,444,425	Apple Inc.
2016/0043751		yes	yes	granted as 9,680,510	Tekcem [P59]
2017/0040704		yes	yes	granted as 10,116,057	Tekcem [P61]
2017/0063344		yes	yes	granted as 9,966,930	Tekcem [P62]

Table 2: cited U.S. patents

	cited in:				
Pat. No.	P63	P69	P70	Inventor	Assigned to
7,260,424	appl*			Schmidt	Intellectual Ventures (US)
8,063,839	yes	yes	yes	Ansari et al.	Quantenna (US)
8,102,830	yes	yes	yes	Yokoi et al.	Samsung (KR)
8,325,097	yes	yes	yes	McKinzie III et al.	Research In Motion RF (US)
9,077,317	appl*	yes	yes	Broyde et al. [P57]	Samsung (KR)
9,444,425			appl*	Mow et al.	Apple Inc. (US)
9,537,223	appl*			Hall et al.	Smart Antenna Technology (UK)
9,621,132		yes	yes	Broyde et al. [P54]	Samsung (KR)
9,654,162		yes	yes	Broyde et al. [P58]	Samsung (KR)
9,680,510		yes	yes	Broyde et al. [P59]	Samsung (KR)
9,698,484		yes	yes	Broyde et al. [P63]	Tekcem (FR)
9,966,930		appl*	appl*	Broyde et al. [P62]	Samsung (KR)
10,116,057		appl*	appl*	Broyde et al. [P61]	Samsung (KR)

* "appl" means that only the US application is cited (refer to Table 1 for the corresponding US application)

Table 3: cited FR patent publications

Pub. No.	Appl. No.	cited in: P63	P69	P70	Applicant
2996067	FR12/02542	yes	yes	yes	Tekcem (FR) [P54]
3004604	FR13/00878	yes			Tekcem (FR) [P57]
3018637	FR14/00606	yes			Tekcem (FR) [P58]
3018973	FR14/00666	yes	yes	yes	Tekcem (FR) [P59]
3021813	FR14/01221	yes	yes	yes	Tekcem (FR) [P60]

Table 4: cited PCT publications

PCT Publication No.	cited in: P63	P69	P70	Applicant
WO 2014/049475	yes	yes	yes	Tekcem (FR) [P54]
WO 2014/170766	yes			Tekcem (FR) [P57]
WO 2015/136409	yes			Tekcem (FR) [P58]
WO 2015/140660	yes	yes	yes	Tekcem (FR) [P59]
WO 2015/181653	yes	yes	yes	Tekcem (FR) [P60]

Hindawi Publishing Corporation
International Journal of Antennas and Propagation
Volume 2016, Article ID 4758486, 15 pages
http://dx.doi.org/10.1155/2016/4758486

Research Article

A Tuning Computation Technique for a Multiple-Antenna-Port and Multiple-User-Port Antenna Tuner

Frédéric Broydé and Evelyne Clavelier

Excem, 12 Chemin des Hauts de Clairefontaine, 78580 Maule, France

Correspondence should be addressed to Evelyne Clavelier; eclavelier@eurexcem.com

Received 27 April 2016; Revised 13 July 2016; Accepted 7 August 2016

Academic Editor: Giuseppe Mazzarella

A multiple-user-port antenna tuner having the structure of a multidimensional π-network has recently been disclosed, together with design equations which assume lossless circuit elements. This paper is about the design of this type of antenna tuner, when losses are taken into account in each circuit element of the antenna tuner. The problem to be solved is the tuning computation, the intended results of which are the reactance values of the adjustable impedance devices of the antenna tuner, which provide an ideal match, if such reactance values exist. An efficient iterative tuning computation technique is presented and demonstrated.

1. Introduction

A multiple-antenna-port and multiple-user-port (MAPMUP) antenna tuner is intended to be inserted between several antennas and a radio device which uses these antennas simultaneously in the same frequency band [1–3]. The radio device may be a receiver, a transmitter, or a transceiver for single-user MIMO radio communication, and the antenna tuner is typically adjusted automatically [4–6]. Figure 1 shows how n antennas may be coupled to a MAPMUP antenna tuner having n antenna ports and m user ports (also referred to as "radio ports") intended to be coupled to the radio device.

In a frequency band of intended operation, with respect to the antenna ports and the user ports, the antenna tuner must behave as a passive linear device and its losses should be as low as possible. The antenna ports see an impedance matrix $\mathbf{Z}_{\text{Sant}}$ of size $n \times n$ and the user ports present an impedance matrix $\mathbf{Z}_U$ of size $m \times m$. A MAPMUP antenna tuner comprises p adjustable impedance devices, each of which may be any component having two terminals which behave as the terminals of a passive linear two-terminal circuit element and which present a reactance which is adjustable by mechanical or electrical means. The function of the antenna tuner is to allow an adjustment of $\mathbf{Z}_U$, using a selection of the reactance values of its adjustable impedance devices, so as to obtain or approximate a wanted impedance matrix $\mathbf{Z}_{UW}$. This tuning capability differentiates a MAPMUP antenna tuner from a MAPMUP matching network [7–13]. Some aspects of the tuning capability of MAPMUP antenna tuners are covered in [14], which shows that the need for a suitable tuning capability (such as a full tuning capability) makes the design of a MAPMUP antenna tuner completely different from the design of a MAPMUP matching network.

A MAPMUP antenna tuner having the structure of a multidimensional π-network has recently been described [14–16]. This antenna tuner is scalable to any $n = m \geq 1$, unlike earlier MAPMUP antenna tuners. It is shown in Figure 2 for the case $n = m = 4$. The case $n = m = 1$ corresponds to a classical single-antenna-port and single-user-port (SAPSUP) antenna tuner having the structure of a π-network.

This paper is about the design of this type of MAPMUP antenna tuner. The problem to be solved is the tuning computation, the intended results of which are the adjustable impedance device reactance values which provide an ideal match $\mathbf{Z}_U = \mathbf{Z}_{UW}$, if such reactance values exist. For a lossless multidimensional π-network antenna tuner, a set of closed-form tuning computation formulas was proven in [16]. In this paper, we shall present an efficient iterative tuning computation technique, which can be used when losses are present in the circuit element of the antenna tuner. Section 2

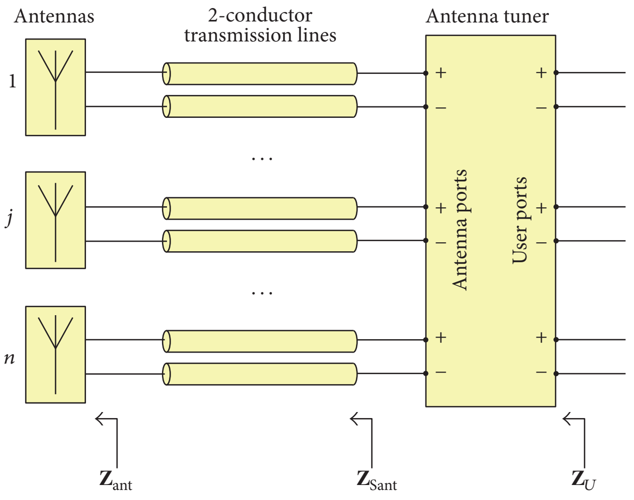

FIGURE 1: An array of n antennas coupled to a MAPMUP antenna tuner through n uncoupled 2-conductor transmission lines.

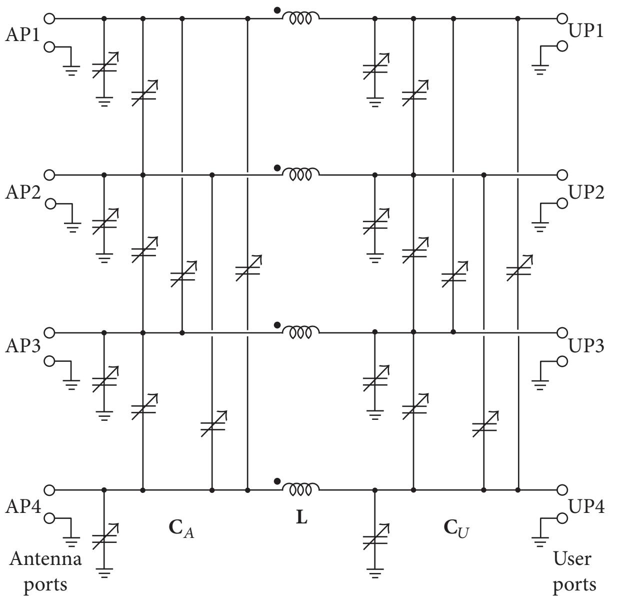

FIGURE 2: The MAPMUP antenna tuner having the structure of a multidimensional π-network, in a configuration having $n = 4$ antenna ports, labeled AP1 to AP4, and $m = 4$ user ports, labeled UP1 to UP4.

presents a tuning computation problem and the solution obtained for a lossless multidimensional π-network antenna tuner. Sections 3 and 4 explain the theory of the iterative algorithm. Sections 5 and 7 present solutions to the problem of Section 2, for different losses in the circuit elements. Sections 6 and 8 explore the main characteristics of the MAPMUP antenna tuner obtained in Section 5.

2. A Tuning Computation Problem

A circular antenna array is made up of $n = 4$ side-by-side parallel dipole antennas, each having a total length of

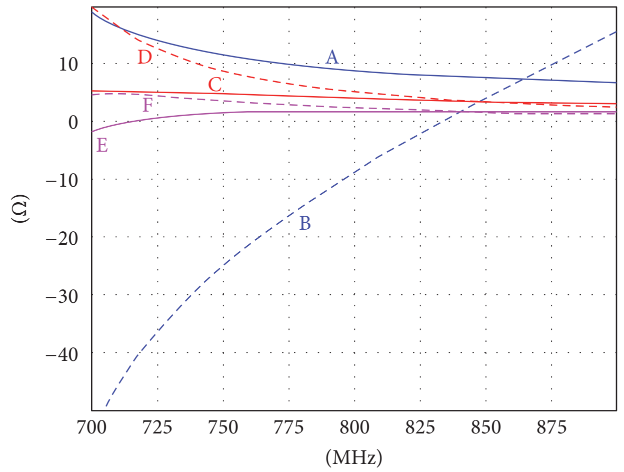

FIGURE 3: Entries of $\mathbf{Z}_{\mathrm{Sant}}$ versus frequency: $\mathrm{Re}(\mathbf{Z}_{\mathrm{Sant}\ 11})$ is curve A; $\mathrm{Im}(\mathbf{Z}_{\mathrm{Sant}\ 11})$ is curve B; $\mathrm{Re}(\mathbf{Z}_{\mathrm{Sant}\ 12})$ is curve C; $\mathrm{Im}(\mathbf{Z}_{\mathrm{Sant}\ 12})$ is curve D; $\mathrm{Re}(\mathbf{Z}_{\mathrm{Sant}\ 13})$ is curve E; $\mathrm{Im}(\mathbf{Z}_{\mathrm{Sant}\ 13})$ is curve F.

224.8 mm. The radius of the array is 56.2 mm. Each antenna is lossless and has a 60 mm long lossy feeder. The antenna array is intended to operate in the frequency band 700 MHz to 900 MHz. At the center frequency $f_c = 800$ MHz, $\mathbf{Z}_{\mathrm{Sant}}$ is approximately given by

$$\mathbf{Z}_{\mathrm{Sant}} \approx \begin{pmatrix} 8.6-8.9j & 3.8+4.9j & 1.7+2.2j & 3.8+4.9j \\ 3.8+4.9j & 8.6-8.9j & 3.8+4.9j & 1.7+2.2j \\ 1.7+2.2j & 3.8+4.9j & 8.6-8.9j & 3.8+4.9j \\ 3.8+4.9j & 1.7+2.2j & 3.8+4.9j & 8.6-8.9j \end{pmatrix} \Omega. \quad (1)$$

At any frequency, $\mathbf{Z}_{\mathrm{Sant}}$ is symmetric and circulant, as shown in (1) at f_c, so that $\mathbf{Z}_{\mathrm{Sant}}$ is fully determined by the first three entries of its first row. These entries are plotted in the frequency range 700 MHz to 900 MHz, in Figure 3.

The MAPMUP antenna tuner of Figure 2 is used to obtain (if possible) that, at any tuning frequency f_T in this frequency range, $\mathbf{Z}_U$ approximates the wanted impedance matrix $\mathbf{Z}_{UW}$, given by

$$\mathbf{Z}_{UW} = r_0 \mathbf{1}_4, \quad (2)$$

where $r_0 = 50\ \Omega$ and where, for a positive integer q, we use $\mathbf{1}_q$ to denote the identity matrix of size $q \times q$.

Let $\mathbf{L}$ be the inductance matrix of the coils shown in Figure 2. Let $\mathbf{C}_A$ and $\mathbf{C}_U$ be the capacitance matrices of the adjustable impedance devices shown on the left and on the right, respectively, in Figure 2. In [16], formulas for the tuning computation were derived, for a lossless multidimensional π-network MAPMUP antenna tuner. In this calculation, one of

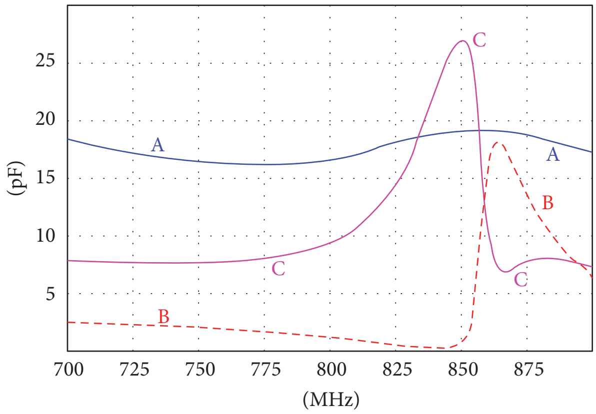

FIGURE 4: Capacitances of the adjustable impedance devices which realize $\mathbf{C}_A$ in the lossless MAPMUP antenna tuner: C_{AG} is curve A; C_{AN} is curve B; and C_{AF} is curve C.

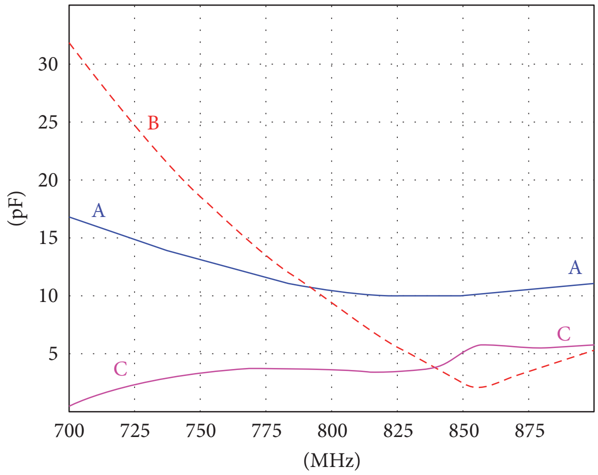

FIGURE 5: Capacitances of the adjustable impedance devices which realize $\mathbf{C}_U$ in the lossless MAPMUP antenna tuner: C_{UG} is curve A; C_{UN} is curve B; and C_{UF} is curve C.

the matrices $\mathbf{L}$, $\mathbf{C}_A$, and $\mathbf{C}_U$ is arbitrary. Let us, for instance, posit

$$\mathbf{L} \approx \begin{pmatrix} 2.700 & 0.760 & 0.850 & 0.760 \\ 0.760 & 2.700 & 0.760 & 0.850 \\ 0.850 & 0.760 & 2.700 & 0.760 \\ 0.760 & 0.850 & 0.760 & 2.700 \end{pmatrix} \text{nH}. \quad (3)$$

The purpose of the tuning computation is to determine values of $\mathbf{C}_A$ and $\mathbf{C}_U$ providing the ideal match $\mathbf{Z}_U = \mathbf{Z}_{UW}$, as a function of the tuning frequency. If we ignore losses in the circuit element of the antenna tuner, we can use (3) and formulas (7) and (9) of [16], to obtain $\mathbf{C}_A$ and $\mathbf{C}_U$. Each value of $\mathbf{C}_A$ is symmetric and circulant. Thus, it corresponds to 3 values of the capacitances of the 10 adjustable impedance devices coupled to one of the antenna ports: C_{AG} for the 4 grounded adjustable impedance devices, C_{AN} for 4 others, and C_{AF} for the 2 remaining ones. These 3 values are plotted in Figure 4, versus the tuning frequency. In the same way, each value of $\mathbf{C}_U$ is symmetric and circulant, so that it corresponds to 3 values of the capacitances of the 10 adjustable impedance devices coupled to one of the user ports: C_{UG} for the 4 grounded adjustable impedance devices, C_{UN} for 4 others, and C_{UF} for the 2 remaining ones. These 3 values are plotted in Figure 5, versus the tuning frequency.

The tuning computation problem addressed in the next sections is the computation, for the MAPMUP antenna tuner of Figure 2, in the presence of losses in the coils and in the adjustable impedance devices, of $\mathbf{C}_A$ and $\mathbf{C}_U$ providing the ideal match $\mathbf{Z}_U = \mathbf{Z}_{UW}$ at different frequencies.

3. Equations of the Tuning Computation Problem

In this section, we present the equations of the tuning computation problem. We use $\mathbf{C}_A$ and $\mathbf{G}_B$ to denote the capacitance and conductance matrices of the $m(m+1)/2$ adjustable impedance devices coupled to one of the antenna ports, so that their admittance matrix is $\mathbf{G}_B + j\omega\mathbf{C}_A$. We use $\mathbf{C}_U$ and $\mathbf{G}_V$ to denote the capacitance and conductance matrices of the $m(m+1)/2$ adjustable impedance devices coupled to one of the user ports, so that their admittance matrix is $\mathbf{G}_V + j\omega\mathbf{C}_U$. We use $\mathbf{L}$ and $\mathbf{R}$ to denote the inductance and resistance matrices of the coils, so that their impedance matrix is $\mathbf{R} + j\omega\mathbf{L}$. Since $\mathbf{C}_A$ and $\mathbf{C}_U$ are adjustable, we consider that $\mathbf{G}_B$ depends on $\mathbf{C}_A$ and on the frequency and that $\mathbf{G}_V$ depends on $\mathbf{C}_U$ and on the frequency. Since different choices of coils at the design stage, to obtain different values of $\mathbf{L}$, entail different losses, we may consider that $\mathbf{R}$ depends on $\mathbf{L}$ and on the frequency.

We use $\mathbf{G}_{\text{Sant}}$ and $\mathbf{B}_{\text{Sant}}$ to denote the conductance matrix and the susceptance matrix seen by the antenna ports so that $\mathbf{Z}_{\text{Sant}}^{-1} = \mathbf{G}_{\text{Sant}} + j\mathbf{B}_{\text{Sant}}$. We see that $\mathbf{Z}_U$ is given by

$$\mathbf{Z}_U = \left[\left[\left[\mathbf{Z}_{\text{Sant}}^{-1} + j\omega\mathbf{C}_A + \mathbf{G}_B \right]^{-1} + j\omega\mathbf{L} + \mathbf{R} \right]^{-1} + j\omega\mathbf{C}_U + \mathbf{G}_V \right]^{-1}. \quad (4)$$

We want to solve the problem of finding $\mathbf{C}_A$, $\mathbf{L}$, and $\mathbf{C}_U$ such that

$$\mathbf{Z}_U = r_0 \mathbf{1}_m, \quad (5)$$

where r_0 is a resistance. The equation to be solved is

$$g_0 \mathbf{1}_m - j\omega\mathbf{C}_U - \mathbf{G}_V = \left[\left[\mathbf{Z}_{\text{Sant}}^{-1} + j\omega\mathbf{C}_A + \mathbf{G}_B \right]^{-1} + j\omega\mathbf{L} + \mathbf{R} \right]^{-1}, \quad (6)$$

where $g_0 = 1/r_0$. Let us introduce the real matrices $\mathbf{G}_T$ and $\mathbf{B}_T$ which satisfy

$$\mathbf{G}_T + j\mathbf{B}_T = \mathbf{Z}_{\text{Sant}}^{-1} + j\omega\mathbf{C}_A + \mathbf{G}_B = \mathbf{G}_{\text{Sant}} + \mathbf{G}_B + j\left[\mathbf{B}_{\text{Sant}} + \omega\mathbf{C}_A\right] \quad (7)$$

so that (6) becomes

$$\begin{aligned} g_0\mathbf{1}_m - j\omega\mathbf{C}_U - \mathbf{G}_V &= \left(j\omega\mathbf{L} + \mathbf{R} + \left[\mathbf{G}_T + j\mathbf{B}_T\right]^{-1}\right)^{-1} \\ &= \left(\left[\mathbf{1}_m + \left(j\omega\mathbf{L} + \mathbf{R}\right)\left(\mathbf{G}_T + j\mathbf{B}_T\right)\right]\left[\mathbf{G}_T + j\mathbf{B}_T\right]^{-1}\right)^{-1} \\ &= \left(\mathbf{G}_T + j\mathbf{B}_T\right) \\ &\cdot \left(\mathbf{1}_m + \mathbf{R}\mathbf{G}_T - \omega\mathbf{L}\mathbf{B}_T + j\left[\mathbf{R}\mathbf{B}_T + \omega\mathbf{L}\mathbf{G}_T\right]\right)^{-1}. \end{aligned} \tag{8}$$

As shown in Appendix of [16], if $\mathbf{M}$ and $\mathbf{N}$ are two square real matrices of size $m \times m$ such that $\mathbf{M} + j\mathbf{N}$ and $\mathbf{M}$ are invertible, we have

$$\left(\mathbf{M} + j\mathbf{N}\right)^{-1} = \left(\mathbf{1}_m - j\mathbf{M}^{-1}\mathbf{N}\right)\left(\mathbf{M} + \mathbf{N}\mathbf{M}^{-1}\mathbf{N}\right)^{-1}. \tag{9}$$

It follows that (8) becomes

$$\begin{aligned} &g_0\mathbf{1}_m - j\omega\mathbf{C}_U - \mathbf{G}_V \\ &\quad = \left(\mathbf{G}_T + j\mathbf{B}_T\right)\left(\mathbf{1}_m - j\mathbf{M}^{-1}\mathbf{N}\right)\left(\mathbf{M} + \mathbf{N}\mathbf{M}^{-1}\mathbf{N}\right)^{-1}, \end{aligned} \tag{10}$$

where

$$\begin{aligned} \mathbf{M} &= \mathbf{1}_m + \mathbf{R}\mathbf{G}_T - \omega\mathbf{L}\mathbf{B}_T \\ \mathbf{N} &= \mathbf{R}\mathbf{B}_T + \omega\mathbf{L}\mathbf{G}_T. \end{aligned} \tag{11}$$

Thus, (6) is equivalent to

$$g_0\mathbf{1}_m - \mathbf{G}_V = \left(\mathbf{G}_T + \mathbf{B}_T\mathbf{M}^{-1}\mathbf{N}\right)\left(\mathbf{M} + \mathbf{N}\mathbf{M}^{-1}\mathbf{N}\right)^{-1} \tag{12}$$

and

$$\omega\mathbf{C}_U = \left(\mathbf{G}_T\mathbf{M}^{-1}\mathbf{N} - \mathbf{B}_T\right)\left(\mathbf{M} + \mathbf{N}\mathbf{M}^{-1}\mathbf{N}\right)^{-1}. \tag{13}$$

At this stage, we have separated the nonlinear complex matrix equation (6) into the coupled nonlinear real matrix equations (12) and (13). For a known $\mathbf{L}$, $\mathbf{R}$ is also known, so that the unknowns are $\mathbf{C}_A$ and $\mathbf{C}_U$. The left-hand sides of (12) and (13) depend only on $\mathbf{C}_U$ and their right-hand sides depend only on $\mathbf{C}_A$. We see that if $\mathbf{G}_V$ was independent of $\mathbf{C}_U$, (12) and (13) would be uncoupled because (12) could be solved to obtain $\mathbf{C}_A$ and (13) could be used to directly compute $\mathbf{C}_U$. Thus, we can say that (12) and (13) are coupled because $\mathbf{G}_V$ depends on $\mathbf{C}_U$. In the case $m = 1$, (12) and (13) may be simplified as shown in Appendix A.

4. Iterative Tuning Computation Technique

An antenna tuner makes sense only if losses are small in the adjustable impedance devices, that is, only if $|||\omega\mathbf{C}_A|||_\infty \gg |||\mathbf{G}_B|||_\infty$, $|||\mathbf{G}_{\mathrm{Sant}}|||_\infty \gg |||\mathbf{G}_B|||_\infty$, $|||\omega\mathbf{C}_U|||_\infty \gg |||\mathbf{G}_V|||_\infty$, and $g_0 \gg |||\mathbf{G}_V|||_\infty$, where $|||\mathbf{A}|||_\infty$ is the maximum row sum matrix norm of a matrix $\mathbf{A}$ [17, § 5.6.5]. Appendix B explains in detail the tuning computation algorithm which will now be concisely presented.

We shall need an equation which gives a possible solution of (12) in the special case $\mathbf{R} = \mathbf{0}\,\Omega$ and $\mathbf{G}_B = \mathbf{G}_V = \mathbf{0}\,$S (that is to say, for a lossless antenna tuner):

$$\mathbf{B}_T = \left(\omega\mathbf{L}\right)^{-1} + \mathbf{G}_A\left[r_0\mathbf{G}_A^{-1}\left(\omega\mathbf{L}\right)^{-2} - \mathbf{1}_m\right]^{1/2}. \tag{14}$$

This equation is a consequence of (B.8) of Appendix B, but it is also equation (26) of [16].

We shall also need an equation derived in Appendix B, which gives a possible general solution of (12):

$$\begin{aligned} \mathbf{B}_T = \left(\omega\mathbf{L}\right)^{-1}\Big(&\mathbf{1}_m + \mathbf{R}\mathbf{G}_T \\ &\pm \mathbf{N}\left[\mathbf{N}^{-1}\left(g_0\mathbf{1}_m - \mathbf{G}_V\right)^{-1}\left(\mathbf{G}_T\mathbf{N}^{-1}\mathbf{M} + \mathbf{B}_T\right)\right. \\ &\left. - \mathbf{1}_m\right]^{1/2}\Big). \end{aligned} \tag{15}$$

In (14) and (15) and in Appendix B, the power 1/2 of a matrix denotes any square root [18, § 6.4.12], such as the primary matrix function associated with a suitable choice of square root in $\mathbb{C}$, this principal matrix function being defined for any nonsingular matrix [18, § 6.2.14]. We note that, unlike (14), (15) cannot be used to directly compute $\mathbf{B}_T$, because

(i) according to (11), $\mathbf{M}$ and $\mathbf{N}$ depend on $\mathbf{B}_T$;

(ii) $\mathbf{G}_V$ depends on $\mathbf{C}_U$ which by (13) depends on $\mathbf{B}_T$;

(iii) by (7), $\mathbf{G}_T$ depends on $\mathbf{G}_B$, which depends on $\mathbf{C}_A$, which again by (7) depends on $\mathbf{B}_T$.

The algorithm is shown in the box "Algorithm 1." At each step $k \geq 0$ in the iteration, there is no guaranty that $\mathbf{C}_A{}^{(k)}$ and $\mathbf{C}_U{}^{(k)}$ are real and that they are positive definite. At each step $k \geq 0$ in the iteration, we compute $F(\mathbf{Z}_U{}^{(k)})$, where we use $\mathbf{Z}_U{}^{(k)}$ to denote the value of $\mathbf{Z}_U$ given by (4) for $\mathbf{C}_A = \mathbf{C}_A{}^{(k)}$, $\mathbf{G}_B = \mathbf{G}_B(\mathbf{C}_A{}^{(k)})$, $\mathbf{C}_U = \mathbf{C}_U{}^{(k)}$, and $\mathbf{G}_V = \mathbf{G}_V(\mathbf{C}_U{}^{(k)})$ and where, for an arbitrary impedance matrix $\mathbf{Z}$ of size $q \times q$, the return figure $F(\mathbf{Z})$ is defined by [14, § VI]

$$F\left(\mathbf{Z}\right) = |||\mathbf{S}\left(\mathbf{Z}\right)|||_2, \tag{16}$$

where

$$\begin{aligned} \mathbf{S}\left(\mathbf{Z}\right) &= \left(\mathbf{Z} + r_0\mathbf{I}_q\right)^{-1}\left(\mathbf{Z} - r_0\mathbf{I}_q\right) \\ &= \left(\mathbf{Z} - r_0\mathbf{I}_q\right)\left(\mathbf{Z} + r_0\mathbf{I}_q\right)^{-1} \end{aligned} \tag{17}$$

and the spectral norm $|||\mathbf{A}|||_2$ of a square matrix $\mathbf{A}$ is the largest singular value of $\mathbf{A}$ [17, § 5.6.6]. A sufficiently small value of $F(\mathbf{Z}_U{}^{(k)})$ ends the iteration. In Algorithm 1, the sufficiently small value is 10^{-4}.

A setting of each adjustable impedance device corresponds to frequency dependent values $\mathbf{C}_A$, $\mathbf{G}_B$, $\mathbf{C}_U$, and $\mathbf{G}_V$. At the end of the algorithm, we compute nominal values of $\mathbf{C}_A$ and $\mathbf{C}_U$, which are frequency independent matrices which correspond to a setting of each adjustable impedance device such that the computed values of $\mathbf{C}_A$ and $\mathbf{C}_U$ are obtained at the frequency of operation.

The selection of different square roots in (14) and (15) can be used to obtain different solutions. Appendix C shows how the iterative algorithm can be simplified in the special case $m = 1$.

Input: frequency of operation, $\mathbf{Z}_{Sant}$.
Output: approximate nominal values of $\mathbf{C}_A$ and $\mathbf{C}_U$, maximal value of the index k, and resulting $F(\mathbf{Z}_U{}^{(k)})$.
(1) compute $\mathbf{C}_A{}^{(0)}$ as the value of $\mathbf{C}_A$ given by (14) and then (7) in which $\mathbf{R} = \mathbf{0}\,\Omega$ and $\mathbf{G}_B = \mathbf{G}_V = \mathbf{0}\,\mathrm{S}$
(2) compute $\mathbf{C}_U{}^{(0)}$ as the value of $\mathbf{C}_U$ given by (7), (11) and (13) in which $\mathbf{R} = \mathbf{0}\,\Omega$, $\mathbf{G}_B = \mathbf{0}\,\mathrm{S}$ and $\mathbf{C}_A = \mathbf{C}_A{}^{(0)}$
(3) $k \leftarrow 0$
(4) compute $F(\mathbf{Z}_U{}^{(0)})$
(5) while $(k < 25) \wedge (F(\mathbf{Z}_U{}^{(k)}) > 10^{-4})$
(6) $\quad k \leftarrow k + 1$
(7) $\quad$ compute $\mathbf{C}_A{}^{(k)}$ as the value of $\mathbf{C}_A$ given by (7), (11) and (15) in which $\mathbf{G}_B = \mathbf{G}_B(\mathbf{C}_A{}^{(k-1)})$ and $\mathbf{G}_V = \mathbf{G}_V(\mathbf{C}_U{}^{(k-1)})$, and in which, except in the left hand side of (15), $\mathbf{C}_A = \mathbf{C}_A{}^{(k-1)}$
(8) $\quad$ compute $\mathbf{C}_U{}^{(k)}$ as the value of $\mathbf{C}_U$ given by (7), (11) and (13) in which $\mathbf{G}_B = \mathbf{G}_B(\mathbf{C}_A{}^{(k-1)})$ and $\mathbf{C}_A = \mathbf{C}_A{}^{(k)}$
(9) $\quad$ compute $F(\mathbf{Z}_U{}^{(k)})$
(10) compute the nominal value of $\mathbf{C}_A$ corresponding to $\mathbf{C}_A{}^{(k)}$ at the frequency of operation
(11) compute the nominal value of $\mathbf{C}_U$ corresponding to $\mathbf{C}_U{}^{(k)}$ at the frequency of operation
(12) return said nominal value of $\mathbf{C}_A$, said nominal value of $\mathbf{C}_U$, k and $F(\mathbf{Z}_U{}^{(k)})$

Algorithm 1: Iterative algorithm for computing approximate nominal values of $\mathbf{C}_A$ and $\mathbf{C}_U$.

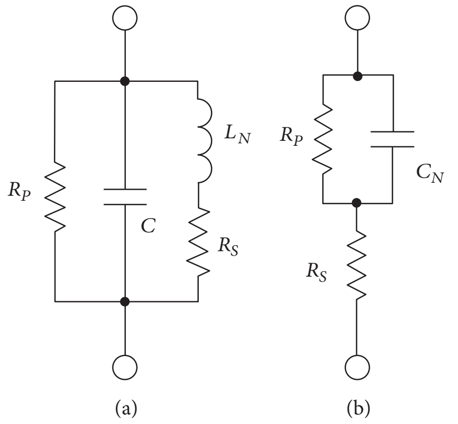

Figure 6: Equivalent circuits (a) for lossy winding of nominal inductance L_N and (b) for a lossy voltage-controlled capacitor of nominal capacitance C_N.

5. First Tuning Computation

We use a lossy coil model based on the equivalent circuit shown in Figure 6(a). According to this model, a winding of nominal inductance L_N has an impedance which is given by

$$Z_L = \frac{1}{(1/(j\omega L_N + R_S)) + j\omega C + (1/R_P)}. \tag{18}$$

In this section, we use $L_N = 2.7\,\mathrm{nH}$, $R_S \approx 119\,\mathrm{m}\Omega$, $R_P \approx 20.7\,\mathrm{k}\Omega$, and $C \approx 48.8\,\mathrm{fF}$, these parameters being realistic for a high-Q coil. Our model of coupled lossy windings has an impedance matrix $\mathbf{Z}_L$ in which the diagonal entries are impedances given by (18) and the nondiagonal entries are produced by frequency independent mutual inductances. We have used

$$\mathbf{Z}_L = j\omega\mathbf{L} + \mathbf{R}$$
$$= Z_L\mathbf{1}_m + j\omega\begin{pmatrix} 0 & 0.76 & 0.85 & 0.76 \\ 0.76 & 0 & 0.76 & 0.85 \\ 0.85 & 0.76 & 0 & 0.76 \\ 0.76 & 0.85 & 0.76 & 0 \end{pmatrix}\mathrm{nH}. \tag{19}$$

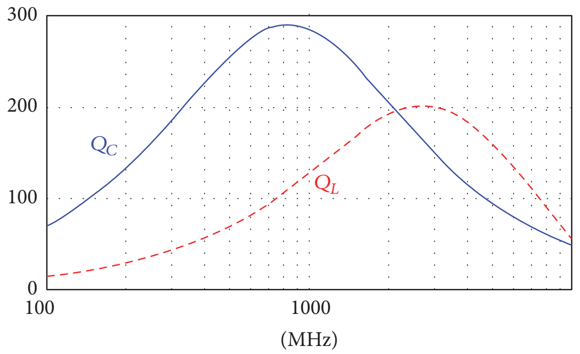

Figure 7: Quality factor Q_L of the diagonal entries of the impedance matrix $\mathbf{Z}_L$ and quality factor Q_C of all entries of the admittance matrix $\mathbf{Y}_C$, for the antenna tuner of Section 5.

Figure 7 shows the quality factor Q_L of the diagonal entries of the impedance matrix $\mathbf{Z}_L$. This quality factor is not very high, since it varies from about 94 to about 117 in the frequency range 700 MHz to 900 MHz.

We use an adjustable impedance device model which is based on the equivalent circuit shown in Figure 6(b).

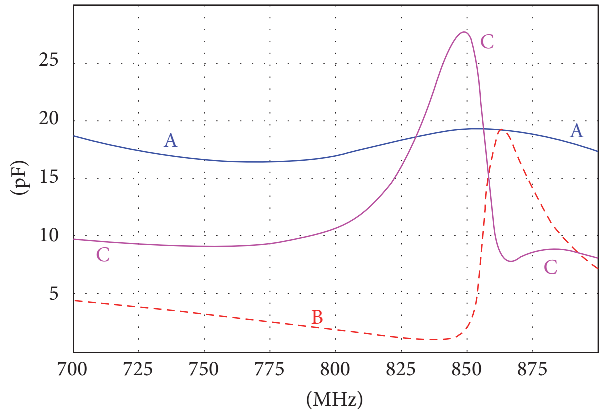

FIGURE 8: Nominal capacitances of the adjustable impedance devices which realize $\mathbf{C}_A$ in the lossy MAPMUP antenna tuner of Section 5, versus the tuning frequency: C_{AG} is curve A; C_{AN} is curve B; and C_{AF} is curve C.

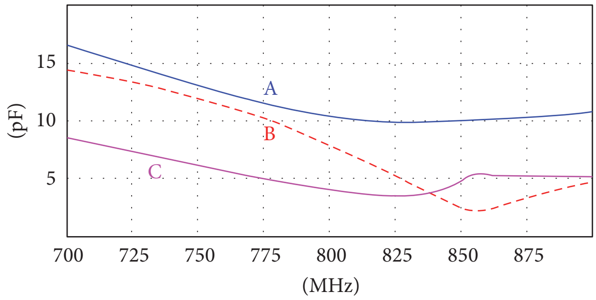

FIGURE 9: Nominal capacitances of the adjustable impedance devices which realize $\mathbf{C}_U$ in the lossy MAPMUP antenna tuner of Section 5, versus the tuning frequency: C_{UG} is curve A; C_{UN} is curve B; and C_{UF} is curve C.

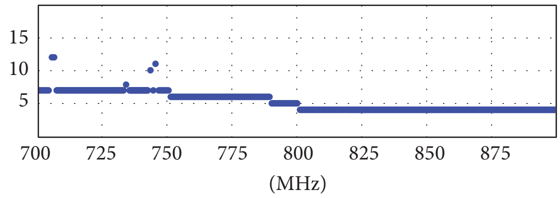

FIGURE 10: Number of iterations used in the tuning computation.

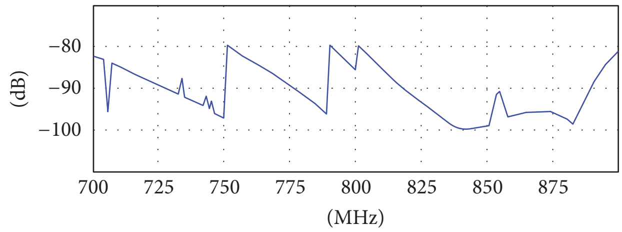

FIGURE 11: The return figure at the end of the tuning computation.

According to this equivalent circuit, a capacitor of nominal capacitance C_N has an admittance which is given by

$$Y_C = \frac{C_N}{\left(1/\left(j\omega + \omega_P\right)\right) + \left(1/\omega_S\right)} \qquad (20)$$

in which $1/R_P = \omega_P C_N$ and $1/R_S = \omega_S C_N$. Thus, the resulting quality factor is independent of the capacitance value. In this section, we use $\omega_P = 9\times 10^6$ rd/s and $\omega_S = 3\times 10^{12}$ rd/s, these parameters being reasonable for high-Q varactors. Figure 7 shows the quality factor Q_C of all entries of the admittance matrix $\mathbf{Y}_C$. In the frequency range 700 MHz to 900 MHz, this quality factor satisfies $284 < Q_C < 289$.

The losses in the coils and adjustable impedance devices are moderate in this frequency range.

To solve the problem set out in Section 2, we have used the iterative algorithm of Section 4 (Algorithm 1) to obtain the nominal values of $\mathbf{C}_A$ and $\mathbf{C}_U$, our program ending the iteration when $F(\mathbf{Z}_U)$ is less than −80 dB. Each computed nominal value of $\mathbf{C}_A$ and $\mathbf{C}_U$ is symmetric and circulant. The nominal capacitances C_{AG}, C_{AN}, and C_{AF} which realize the nominal value of $\mathbf{C}_A$, as explained in Section 2, are plotted in Figure 8, versus the tuning frequency. The nominal capacitances C_{UG}, C_{UN}, and C_{UF} which realize the nominal value of $\mathbf{C}_U$, as explained in Section 2, are plotted in Figure 9 versus the tuning frequency. The number of iterations used in the algorithm (i.e., the maximum value of k) at each tuning frequency is shown in Figure 10, and the corresponding return figure $F(\mathbf{Z})$ is shown in Figure 11. A comparison of Figure 8 with Figure 4 and of Figure 9 with Figure 5 shows large differences for $\mathbf{C}_U$ below 800 MHz. This indicates that moderate losses may strongly modify the results of the tuning computation.

Instead of an iterative algorithm, we can also consider a brute force numerical optimization to perform the tuning computation. For instance, it is possible to use $\mathbf{C}_A = \mathbf{C}_A{}^{(0)}$ and $\mathbf{C}_U = \mathbf{C}_U{}^{(0)}$ as the initial value of an optimization of the capacitances $C_{A1}, \ldots, C_{Ah}$ of the capacitors which produce $\mathbf{C}_A$ and of the capacitances $C_{U1}, \ldots, C_{Uh}$ of the capacitors which produce $\mathbf{C}_U$, to minimize $F(\mathbf{Z}_U)$ and obtain

$$\left(C_{A1}, \ldots, C_{Ah}, C_{U1}, \ldots, C_{Uh}\right) = \underset{C_{Ai}>0,\, C_{Uj}>0}{\arg\min}\ F\left(\mathbf{Z}_U\right). \qquad (21)$$

In the present case, since the symmetry of our problems requires that $\mathbf{C}_A$ and $\mathbf{C}_U$ are symmetric and circulant, we only need to consider an optimization of the 6 parameters C_{AG}, C_{AN}, C_{AF}, C_{UG}, C_{UN}, and C_{UF} defined above. We have also applied this approach to our example, using a commercially available nonlinear numerical solver, at a single frequency, because the convergence is slow. At this frequency (800 MHz), the solver does not reach the exact solution $F(\mathbf{Z}_U) = 0$, but it finds an approximate solution for which $F(\mathbf{Z}_U)$ is about −64 dB.

Moreover, if the problem did not have a rotational symmetry, the optimization approach would become unpractical, because a 20-parameter optimization would be needed (subject to the so-called "curse of dimensionality"). In contrast, the proposed iterative algorithm is unaffected by a lack of symmetry.

6. Performance of the Antenna Tuner

Let us first consider that the antenna tuner and the antennas are used for emission, a multiport source of internal impedance matrix $\mathbf{Z}_S$ being connected to the user ports. The insertion gain of the antenna tuner evaluated for $\mathbf{Z}_S = r_0\mathbf{1}_m$, denoted by G_I, is given by

$$G_I = \left.\frac{P_{\text{out}}}{P_{\text{WAT}}}\right|_{\mathbf{Z}_S = r_0\mathbf{1}_m}, \tag{22}$$

where P_{out} is the power delivered by the antenna ports of the antenna tuner to the antennas and P_{WAT} is the power received by the antennas if the antenna tuner is not present, that is, if the antennas are directly connected to the multiport source. The insertion gain is a significant measure of the benefits of the antenna tuner.

The transducer power gain of the antenna tuner evaluated for $\mathbf{Z}_S = r_0\mathbf{1}_m$, denoted by G_T, is defined as

$$G_T = \left.\frac{P_{\text{out}}}{P_{\text{ava}}}\right|_{\mathbf{Z}_S = r_0\mathbf{1}_m}, \tag{23}$$

where P_{ava} denotes the power available from the multiport source. The antenna tuner being passive, we have $G_T \leq 1$. At the tuning frequency, if $\mathbf{Z}_U$ closely approximates a wanted impedance matrix providing maximum power transfer (as is the case in Section 5, according to Figure 11), then the power received by the user ports of the antenna tuner is near P_{ava}. In this case, G_T is the efficiency of the antenna tuner.

We may define a mismatch factor without the antenna tuner evaluated for $\mathbf{Z}_S = r_0\mathbf{1}_m$, denoted by M_{WAT} and given by

$$M_{\text{WAT}} = \left.\frac{P_{\text{WAT}}}{P_{\text{ava}}}\right|_{\mathbf{Z}_S = r_0\mathbf{1}_m}. \tag{24}$$

Here, G_I, G_T, and M_{WAT} are functions of the column vector of the open-circuit voltages of the source, denoted by $\mathbf{V}_0$. More precisely G_I, G_T, and M_{WAT} are ratios of Hermitian forms of $\mathbf{V}_0$. In the case where $\mathbf{V}_0$ is known, G_I, G_T, and M_{WAT} can be computed. In the case where $\mathbf{V}_0$ is not known, it may be considered as random complex vectors. In this case, if we had suitable information on the statistics of $\mathbf{V}_0$, we could derive the expectations of G_I, G_T, and M_{WAT}. It directly follows from (22)–(24) that

$$G_I = \frac{G_T}{M_{\text{WAT}}}. \tag{25}$$

Using an antenna tuner is advantageous from the insertion gain standpoint if and only if $G_I > 1$. Since $G_T \leq 1$, by (25) the use of an antenna tuner only makes sense if M_{WAT} is sufficiently low. In Figure 12, we have plotted G_I, G_T, and M_{WAT} as a function of the tuning frequency, for the tuning solution shown in Figures 8 and 9, and for $\mathbf{V}_0$ equal to $\mathbf{V}_{01}$ or $\mathbf{V}_{02}$ or $\mathbf{V}_{03}$ or $\mathbf{V}_{04}$ given by

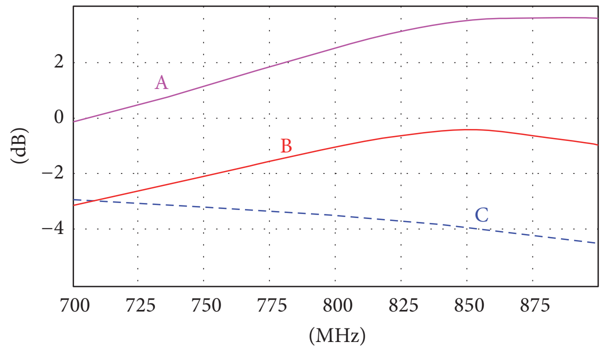

Figure 12: Insertion gain (curve A), transducer power gain (curve B), and mismatch factor without the antenna tuner (curve C).

$$\mathbf{V}_{01} = \begin{pmatrix} 2 \\ 0 \\ 0 \\ 0 \end{pmatrix} \text{V}; \quad \mathbf{V}_{02} = \begin{pmatrix} 0 \\ 2 \\ 0 \\ 0 \end{pmatrix} \text{V}; \quad \mathbf{V}_{03} = \begin{pmatrix} 0 \\ 0 \\ 2 \\ 0 \end{pmatrix} \text{V}; \quad \mathbf{V}_{04} = \begin{pmatrix} 0 \\ 0 \\ 0 \\ 2 \end{pmatrix} \text{V} \tag{26}$$

or to any multiple of any one of these vectors. The relationship (25) is visible in Figure 12. Since the insertion gain is greater than 0 dB in most of the frequency band 700 MHz to 900 MHz, this antenna tuner does not seem ridiculous from the insertion gain standpoint.

For $\alpha \in \{1, \ldots, 4\}$, let $\mathbf{E}_{0\alpha}$ be the electric field radiated by the antenna array in a configuration where $\mathbf{Z}_S = r_0\mathbf{1}_m$ and $\mathbf{V}_0$ is equal to $\mathbf{V}_{0\alpha}$ given by (26), in which rms values are used. A plot of the average radiation intensity of $\mathbf{E}_{0\alpha}$ in the far field, as a function of an angle, may be referred to as a radiation pattern of user port α. Let us use a spherical coordinate system having an origin at the center of the dipole centers and a z-axis parallel to the direction of the parallel dipoles, θ being the zenith angle (i.e., the angle with respect to the z-axis) and φ being the azimuth angle, with respect to the first antenna. Thus, the dipole centers are in the plane

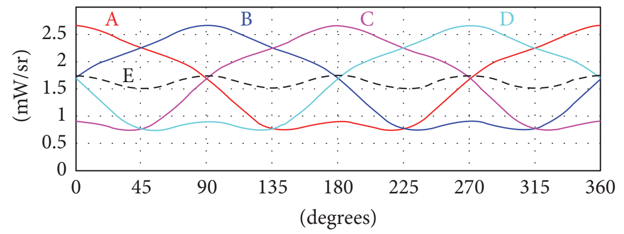

Figure 13: Radiation patterns of the user ports, at 800 MHz, in the plane $\theta = \pi/2$, versus the azimuth angle φ: the pattern of user port 1 is curve A; the pattern of user port 2 is curve B; the pattern of user port 3 is curve C; the pattern of user port 4 is curve D; and the average of curves A to D is curve E.

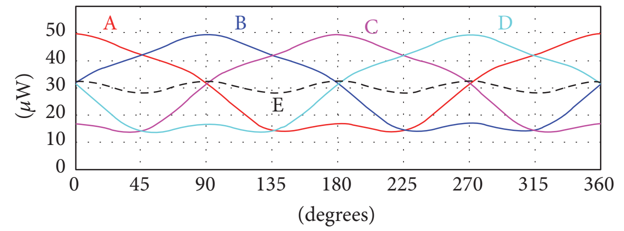

Figure 14: Reception patterns of the user ports, at 800 MHz, in the plane $\theta = \pi/2$, versus the azimuth angle φ: the pattern of user port 1 is curve A; the pattern of user port 2 is curve B; the pattern of user port 3 is curve C; the pattern of user port 4 is curve D; and the average of curves A to D is curve E.

$\theta = \pi/2$ orthogonal to the dipole antennas, which is their plane of maximum far field radiation, and the azimuths of the centers of antennas 1 to 4 are 0, $\pi/2$, π, and $3\pi/2$, respectively. Figure 13 shows the radiation patterns of the user ports, for a tuning frequency of 800 MHz and at this frequency, in the plane $\theta = \pi/2$, versus φ.

Let $\mathbf{P}_R$ be the matrix of the self- and cross and complex powers radiated by the antenna array over all values of θ and φ, defined as follows: for $\alpha \in \{1, \ldots, 4\}$ and $\beta \in \{1, \ldots, 4\}$, the entry $P_{R\alpha\beta}$ of $\mathbf{P}_R$ is given by

$$P_{R\alpha\beta} = \frac{1}{\eta_0} \int_0^{\pi} \int_0^{2\pi} \mathbf{E}_{0\alpha}^{*} \mathbf{E}_{0\beta} r^2 \sin\theta \, d\varphi \, d\theta, \tag{27}$$

where $\eta_0 \approx 376.7\,\Omega$ is the intrinsic impedance of free space, where $\mathbf{E}_{0\alpha}$ and $\mathbf{E}_{0\beta}$ are regarded as column vectors, where the star denotes the Hermitian adjoint, and where the integration is carried out at a large distance r from the antennas lying in free space. Using a numerical integration, at 800 MHz, we obtain

$$\mathbf{P}_R \approx \begin{pmatrix} 10.872 & 3.350 & -0.320 & 3.350 \\ 3.350 & 10.872 & 3.350 & -0.320 \\ -0.320 & 3.350 & 10.872 & 3.350 \\ 3.350 & -0.320 & 3.350 & 10.872 \end{pmatrix} \text{mW}. \tag{28}$$

Here, the available power of 20 mW, corresponding to any one of the $\mathbf{V}_{0\alpha}$ given by (26), leads to a power of about 15.756 mW at the output of the antenna tuner (in line with the value of G_T shown in Figure 12), but only 10.872 mW reaches the antennas and is radiated, because of feeder loss. The feeder loss of about 1.61 dB is much larger than the product of the feeder attenuation constant and the feeder length, equal to 0.20 dB at 800 MHz. This effect is similar to, but more complex than, the additional feeder loss caused by the high standing-wave ratio associated with the use of SAPSUP antenna tuners [19, ch. 3].

Since, by (27), $P_{R\alpha\beta}$ is an inner product [17, § 0.6.4] of the beams $\mathbf{E}_{0\beta}$ and $\mathbf{E}_{0\alpha}$, we can define the beam cosines $\rho_{\alpha\beta} = P_{R\alpha\beta}/(P_{R\alpha\alpha}P_{R\beta\beta})^{1/2}$ of $\mathbf{P}_R$. At 800 MHz, the matrix of these beam cosines is given by

$$\left(\rho_{\alpha\beta}\right) \approx \begin{pmatrix} 1.000 & 0.308 & -0.029 & 0.308 \\ 0.308 & 1.000 & 0.308 & -0.029 \\ -0.029 & 0.308 & 1.000 & 0.308 \\ 0.308 & -0.029 & 0.308 & 1.000 \end{pmatrix}. \tag{29}$$

Let us now consider that the antenna tuner and the antennas are used for reception, a multiport load of impedance matrix $\mathbf{Z}_L$ being connected to the user ports. Let $\mathbf{U}_0$ be the column vector of the rms voltages delivered by the user ports in a configuration where $\mathbf{Z}_L = r_0 \mathbf{1}_m$ and a plane wave of electric field amplitude 1 V/m rms impinges on the antenna array, from the direction (θ, φ) with an electric field lying in a plane containing the z-axis. A plot of the average power delivered by the user port α, as a function of an angle, may be referred to as a reception pattern of user port α. Figure 14 shows the reception patterns of the user ports, for a tuning frequency of 800 MHz and at this frequency, in the plane $\theta = \pi/2$, versus φ. The shapes of the reception patterns of the user ports correspond to those of the radiation patterns of the user ports. This is because, for each user port, the reception pattern and the radiation pattern correspond to the directivity pattern of a single-port antenna made up of all items shown in Figure 1, plus 50 Ω resistors connected to the other user ports.

Let $\mathbf{P}_D$ be the matrix of the self- and cross and complex powers delivered by the user ports, averaged over all values of θ and φ, defined as follows: for $\alpha \in \{1, \ldots, 4\}$ and $\beta \in \{1, \ldots, 4\}$, the entry $P_{D\alpha\beta}$ of $\mathbf{P}_D$ is given by

$$P_{D\alpha\beta} = \frac{1}{4\pi r_0} \int_0^{\pi} \int_0^{2\pi} U_{0\alpha} \overline{U}_{0\beta} \sin\theta \, d\varphi \, d\theta, \tag{30}$$

where the bar indicates the complex conjugate and where $U_{0\alpha}$ and $U_{0\beta}$ are entries of $\mathbf{U}_0$. Thus, it is possible to write

$$\mathbf{P}_D = \frac{1}{4\pi r_0} \int_0^{\pi} \int_0^{2\pi} \mathbf{U}_0 \mathbf{U}_0^{*} \sin\theta \, d\varphi \, d\theta. \tag{31}$$

Using a numerical integration of (31), we get

$$\mathbf{P}_D \approx \begin{pmatrix} 16.125 & 4.969 & -0.475 & 4.969 \\ 4.969 & 16.125 & 4.969 & -0.475 \\ -0.475 & 4.969 & 16.125 & 4.969 \\ 4.969 & -0.475 & 4.969 & 16.125 \end{pmatrix} \mu\text{W}. \quad (32)$$

The trace of $\mathbf{P}_D$ is the power delivered by the user ports, averaged over all directions of arrival of a plane wave of electric field amplitude 1 V/m rms impinging on the antenna array.

Since, by (30), $P_{D\alpha\beta}$ is an inner product of the beams $U_{0\alpha}$ and $U_{0\beta}$, we can define the beam cosines $P_{D\alpha\beta}/(P_{D\alpha\alpha}P_{D\beta\beta})^{1/2}$ of $\mathbf{P}_D$. In our configuration, the beam cosines of $\mathbf{P}_D$ are equal to the beam cosines of $\mathbf{P}_R$, so that they are, at 800 MHz, given by (29). We note that these beam cosines are similar to, but different from, the correlation coefficients given by (29) or (30) of [20]. The beam cosines are sometimes referred to as "orthogonality coefficients." The values of the beam cosines indicate that the beams are not far from being orthogonal, but they are not orthogonal either.

We have checked that if we remove the losses of the feeders and perform a new tuning computation for a lossless antenna tuner, we obtain a matrix of the beam cosines equal to $\mathbf{1}_4$, as requested by the theory presented in [21, 22].

7. Second Tuning Computation

We now use different parameters in the loss models of Section 5: $L_N = 2.7$ nH, $R_S = 0.36\,\Omega$, $R_P \approx 10.1$ kΩ, $C \approx 93.8$ fF, $\omega_P = 37 \times 10^6$ rd/s, and $\omega_S = 650 \times 10^9$ rd/s.

Figure 15 shows the quality factor Q_L of the diagonal entries of the impedance matrix $\mathbf{Z}_L$. Unfortunately, this quality factor is not high, since it varies from about 31.6 to about 39.5 in the frequency range 700 MHz to 900 MHz. Figure 15 also shows the quality factor Q_C of all entries of the admittance matrix $\mathbf{Y}_C$. In the frequency range 700 MHz to 900 MHz, this quality factor is close to 66. Thus, the losses in the coils and adjustable impedance devices are higher than in Section 5 and very substantial. This is good for testing our iterative algorithm, because higher losses are less favorable for convergence.

We have again used the iterative algorithm of Section 4 (Algorithm 1) to obtain $\mathbf{C}_A$ and $\mathbf{C}_U$, our program ending the iteration when $F(\mathbf{Z}_U)$ is less than −80 dB. The number of iterations needed to obtain this required accuracy at each tuning frequency is shown in Figure 16, and the corresponding return figure $F(\mathbf{Z})$ is shown in Figure 17. A comparison of Figure 10 with Figure 16 shows that the number of iterations has increased. However, the algorithm still converges rapidly.

In Figure 18, we have plotted G_I, G_T, and M_{WAT} as a function of the tuning frequency, for the tuning solution obtained here, and for $\mathbf{V}_0$ equal to $\mathbf{V}_{01}$ or $\mathbf{V}_{02}$ or $\mathbf{V}_{03}$ or $\mathbf{V}_{04}$ given by (26) or to any multiple of any one of these vectors. A comparison of Figure 12 with Figure 18 shows that G_I and G_T have decreased. Since the insertion gain is below 0 dB below about 790 MHz, this antenna tuner is not satisfactory from the insertion gain standpoint.

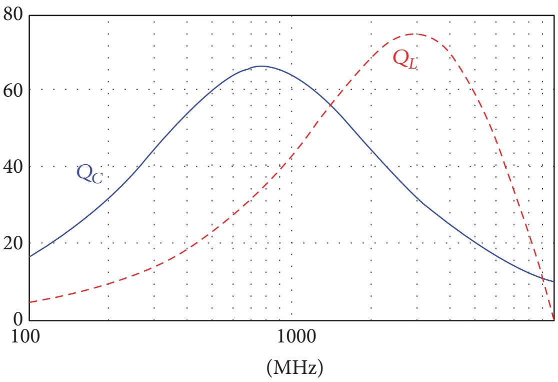

FIGURE 15: Quality factor Q_L of the diagonal entries of the impedance matrix $\mathbf{Z}_L$ and quality factor Q_C of all entries of the admittance matrix $\mathbf{Y}_C$, for the antenna tuner of Section 7.

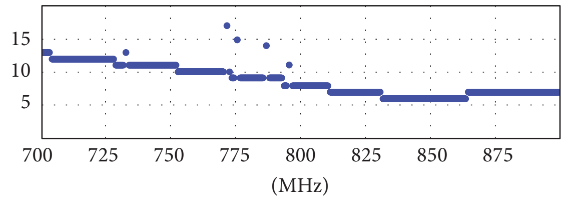

FIGURE 16: Number of iterations used in the tuning computation.

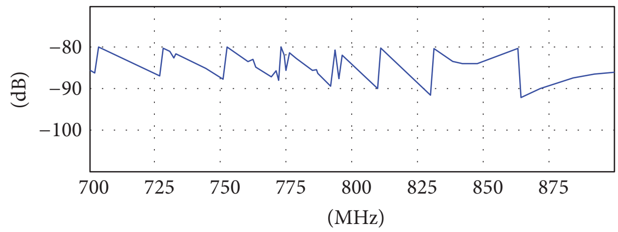

FIGURE 17: The return figure at the end of the tuning computation.

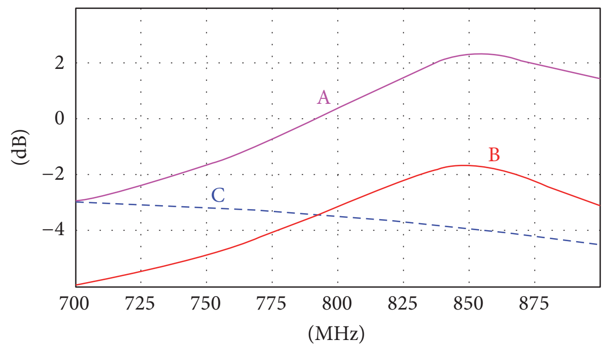

FIGURE 18: Insertion gain (curve A), transducer power gain (curve B), and mismatch factor without the antenna tuner (curve C).

8. Effects of Capacitance Deviations

To ensure that the tuning computation technique is applicable to real components, we now study the criticality of the

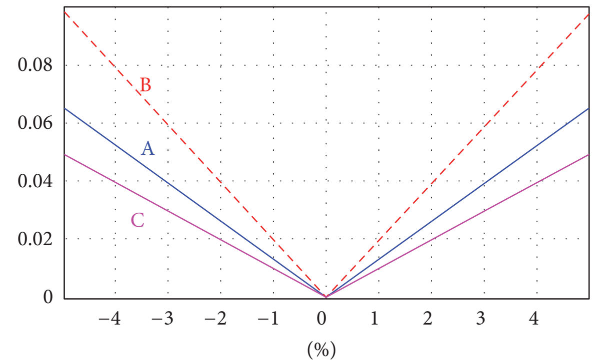

Figure 19: $F(\mathbf{Z}_U)$ at the tuning frequency, versus a relative capacitance variation of a single adjustable impedance device contributing to $\mathbf{C}_U$: curve A if its initial value is C_{UG}; curve B if its initial value is C_{UN}; curve C if its initial value is C_{UF}.

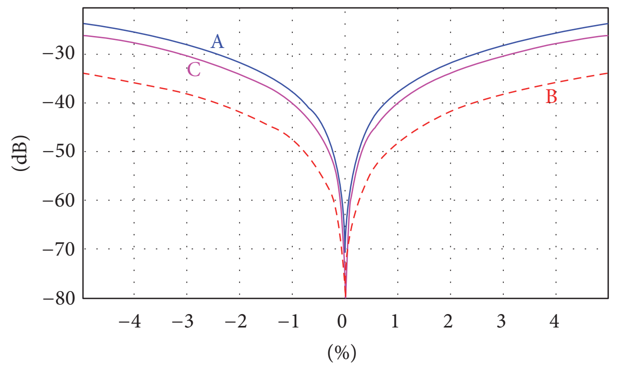

Figure 20: $F(\mathbf{Z}_U)$ in dB at the tuning frequency, versus a relative capacitance variation of a single adjustable impedance device contributing to $\mathbf{C}_A$: curve A if its initial value is C_{AG}; curve B if its initial value is C_{AN}; curve C if its initial value is C_{AF}.

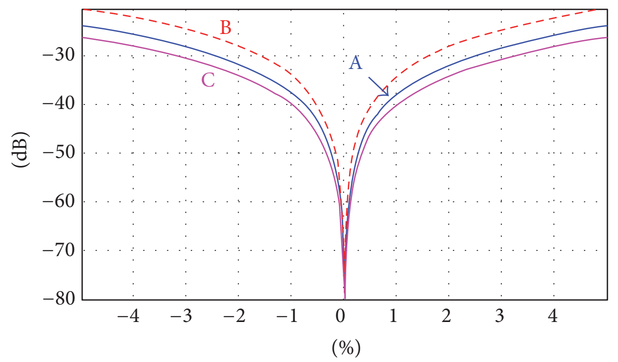

Figure 21: $F(\mathbf{Z}_U)$ in dB at the tuning frequency, versus a relative capacitance variation of a single adjustable impedance device contributing to $\mathbf{C}_U$: curve A if its initial value is C_{UG}; curve B if its initial value is C_{UN}; curve C if its initial value is C_{UF}.

calculated values, for the MAPMUP antenna tuner designed in Section 5. We consider deviations of one or more of the capacitances of its 20 adjustable impedance devices, from the computed ones, and we investigate the effects of the deviations on the return figure $F(\mathbf{Z}_U)$ at 800 MHz, for a tuning frequency of 800 MHz.

Since, at the tuning frequency, $F(\mathbf{Z}_U)$ practically reaches its minimum value of 0, it would, if it was differentiable, have all its partial derivatives with respect to the capacitances practically equal to zero, at the tuning frequency. Thus, each of the 20 absolute sensitivities of $F(\mathbf{Z}_U)$ with respect to the capacitance of one of the adjustable impedance devices would practically be zero, at the tuning frequency [23, ch. 68]. Figure 19 shows $F(\mathbf{Z}_U)$ at the tuning frequency, as a function of a relative capacitance variation of a single adjustable impedance device contributing to $\mathbf{C}_U$. All curves of Figure 19 have a corner point at zero relative capacitance variation. The same phenomenon occurs in plots of $F(\mathbf{Z}_U)$ at the tuning frequency, as a function of a relative capacitance variation of a single adjustable impedance device contributing to $\mathbf{C}_A$. For much smaller capacitance variations, the corner points vanish, but no useful absolute or relative sensitivity with respect to the capacitances of the adjustable impedance devices can be defined.

Figures 20 and 21 show $F(\mathbf{Z}_U)$ in dB, at the tuning frequency, as a function of a relative capacitance variation of a single adjustable impedance device contributing to $\mathbf{C}_A$ or to $\mathbf{C}_U$.

To obtain a better idea of the effect of simultaneous deviations of the capacitance of the 20 adjustable impedance devices, we have assumed independent normally distributed capacitance deviations, with a zero mean deviation from the computed values, and a specified relative standard deviation σ_C. At the tuning frequency, we have determined the statistic of $F(\mathbf{Z}_U)$ in dB, the mean of $F(\mathbf{Z}_U)$ in dB, denoted by m_F, and the corrected sample standard deviation of $F(\mathbf{Z}_U)$ in dB, denoted by σ_F. The histogram of Figure 22 shows the relative frequency of $F(\mathbf{Z}_U)$ in dB obtained for $\sigma_C = 1\%$, with 10000 samples (of the MAPMUP antenna tuner). The assumption $\sigma_C = 1\%$ could, for instance, correspond to a ±3% tolerance defined by a 3-sigma deviation. For the statistics shown in Figure 22, we have $m_F \approx -27.22$ dB and $\sigma_F \approx 2.79$ dB. The minimum value of $F(\mathbf{Z}_U)$ is −39.96 dB. It is remarkable that this minimum value is not closer to the lowest possible value of about −85.68 dB shown in Figure 11 for 800 MHz. This is because each sample comprises 20 normally distributed capacitances, so that the probability of having all of these capacitances close to their respective computed values is very small. The maximum value of $F(\mathbf{Z}_U)$ is −19.00 dB, whereas for a normal distribution the probability of having $F(\mathbf{Z}_U)$ greater than $m_F + 3\sigma_F \approx -18.86$ dB would be about 1.35×10^{-3}, corresponding to an expectation of about 13.5 for 10000 samples. Figure 23 shows m_F and σ_F, as a function of σ_C, obtained with 1000 samples for each value of σ_C.

Based on the foregoing, we may conclude that a specified maximum return figure of $m_F + 3\sigma_F \approx -18.86$ dB at the tuning frequency can reliably be obtained with $\sigma_C \leq 1\%$. This value of $m_F + 3\sigma_F$ is less impressive than the return figures below −80 dB shown in Figure 11. However, this specified maximum return figure can be compared to a reasonable design target −10 dB for a wireless transmitter and to the return figure achievable with an alternative antenna tuner made up of 4

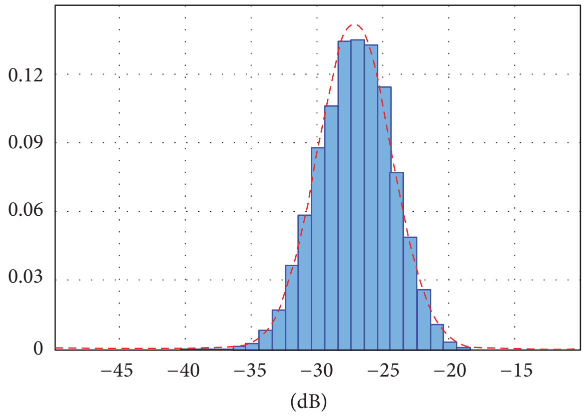

FIGURE 22: Histogram of the relative frequency of $F(\mathbf{Z}_U)$ in dB, for $\sigma_C = 1\%$, obtained with 10000 samples, and normal distribution having the same mean and the same standard deviation (dashed curve).

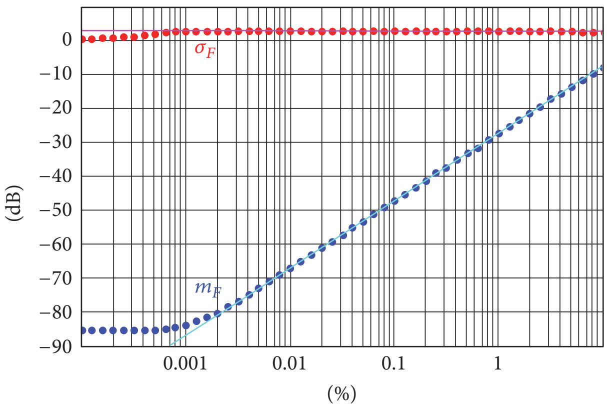

FIGURE 23: m_F and σ_F versus σ_C and linear regression lines based on the values obtained for $0.01\% \le \sigma_C \le 10\%$.

independent and uncoupled SAPSUP antenna tuners each having the structure of a π-network. Such an antenna tuner corresponds to the schematic diagram of Figure 2, with the constraint that $\mathbf{C}_A$, $\mathbf{L}$, and $\mathbf{C}_U$ are diagonal matrices. Using the same L_N and Y_C as in Section 5, we obtain, for this alternative antenna tuner, a minimum return figure of −5.90 dB at 800 MHz, obtained for nominal values of C_{AG} and C_{UG}, respectively, equal to about 25.36 pF and 24.02 pF. Thus, the specified maximum return figure is much better than the return figure achievable with the alternative antenna tuner using optimum capacitances.

The antenna tuners considered in this paper are typically intended to be adjusted automatically. In an automatic tuning system using closed-loop control, like the ones considered in [4–6], deviations of the adjustable impedance device capacitances caused by manufacturing tolerances, temperature, or other external causes may be automatically compensated. This is not the case in an automatic tuning system using open-loop control, like the ones considered in [24–26]. With open-loop control, the effects of component value variations are crucial, because they are not inherently compensated.

9. Conclusion

We have studied the design of a MAPMUP antenna tuner having the structure of a multidimensional π-network, when losses are taken into account in all circuit elements of the antenna tuner. Our work also covers a SAPSUP having the structure of a π-network. The main aspect that we have addressed is the tuning computation, the intended results of which are the adjustable impedance device reactance values which provide an ideal match of the antenna tuner, if such reactance values exist.

An efficient iterative tuning computation technique was explained and demonstrated in two examples. It can be used with circuit element losses depending in any way on the frequency and on the reactance of the circuit element. In the examples used to demonstrate the iterative tuning computation algorithm, we have chosen to use moderate losses in the first example and higher losses in the second example. The algorithm converges rapidly in both cases, but the speed decreases with increased losses. We have found that moderate losses may substantially modify the results of the tuning computation. In other words, the adjustable impedance device reactance values which provide an ideal match may, in the presence of moderate losses, be significantly different from what they would be if losses were not present.

The fact that the iterative tuning computation technique converges shows that the multidimensional π-network antenna tuner may be able to provide an ideal match $\mathbf{Z}_U = r_0 \mathbf{1}_m$ which realizes decoupling and matching. In the investigated examples, this is obtained at any frequency in a wide frequency band of intended operation. The iterative tuning computation technique can be used as a tool to design π-network and multidimensional π-network antenna tuners. In addition, it can be used in automatic tuning systems based on an open-loop control scheme, such as the ones described in [24–26], to obtain the tuning control signals which determine the reactance of each of the adjustable impedance devices.

The design of a MAPMUP antenna tuner is a new field, with many unanswered questions. For instance, the selection of the inductance values of π-network and multidimensional π-network antenna tuners has not been addressed in this paper, since we have solved (12) and (13) for a known $\mathbf{L}$. The literature in this area is limited to SAPSUP π-network antenna tuners, and available design techniques (except optimization using a general-purpose circuit optimizer, which is extremely slow) ignore losses in the circuit elements of the antenna tuner or do not fully take them into account [27, 28]. We believe that this work could also be used to solve this problem, for multidimensional π-network antenna tuners, with arbitrary losses.

Appendix

A. Equations of the Tuning Computation Problem for a SAPSUP Antenna Tuner

In the case of a π-network SAPSUP antenna tuner, the results of Section 3 may be simplified as follows. Here, the antenna port sees an impedance Z_{Sant} and the user port presents an impedance Z_U. We use C_A and G_B to denote the capacitance and the conductance of the adjustable impedance device coupled to the antenna port, so that its admittance is $G_B + j\omega C_A$. We use C_U and G_V to denote the capacitance and the conductance of the adjustable impedance device coupled to the user port, so that its admittance is $G_V + j\omega C_U$. We use L and R to denote the inductance and the resistance of the coil, so that its impedance is $R + j\omega L$. We consider that G_B depends on C_A and on the frequency, G_V depends on C_U and on the frequency, and R depends on L and on the frequency.

We use G_{Sant} and B_{Sant} to denote the conductance and the susceptance seen by the antenna port, so that $1/Z_{\text{Sant}} = G_{\text{Sant}} + jB_{\text{Sant}}$. Here, (4) becomes

$$Z_U = \left(\left(\left(Z_{\text{Sant}}^{-1} + j\omega C_A + G_B\right)^{-1} + j\omega L + R\right)^{-1} + j\omega C_U + G_V\right)^{-1}. \tag{A.1}$$

We want to solve the problem of finding C_A, L, and C_U such that Z_U is equal to a wanted resistance r_0. The equation to be solved is

$$g_0 - j\omega C_U - G_V = \left(\left(Z_{\text{Sant}}^{-1} + j\omega C_A + G_B\right)^{-1} + j\omega L + R\right)^{-1}. \tag{A.2}$$

Let us introduce the reals G_T and B_T which satisfy

$$\begin{aligned} G_T + jB_T &= \frac{1}{Z_{\text{Sant}}} + j\omega C_A + G_B \\ &= G_{\text{Sant}} + G_B + j\left[B_{\text{Sant}} + \omega C_A\right]. \end{aligned} \tag{A.3}$$

We find that (A.2) is equivalent to

$$g_0 - G_V = \frac{G_T + R\left(G_T^2 + B_T^2\right)}{\left(1 + RG_T - \omega LB_T\right)^2 + \left(RB_T + \omega LG_T\right)^2}, \tag{A.4}$$

$$\omega C_U = \frac{\omega L\left(G_T^2 + B_T^2\right) - B_T}{\left(1 + RG_T - \omega LB_T\right)^2 + \left(RB_T + \omega LG_T\right)^2} \tag{A.5}$$

which replace (12) and (13).

B. Derivation of a Tuning Computation Technique for a MAPMUP Antenna Tuner

In the case of a multidimensional π-network MAPMUP antenna tuner, the results of Section 4 may be established as follows.

Assuming that losses are small in the adjustable impedance devices, an iterative algorithm could in principle be used to solve (12) and (13): at each iteration of this algorithm, $\mathbf{C}_A$ and $\mathbf{C}_U$ are determined using (12) and (13), respectively, in which $\mathbf{G}_B$ and $\mathbf{G}_V$ are regarded as constants which are updated at each iteration, based on the values of $\mathbf{C}_A$ and $\mathbf{C}_U$ determined at the previous iteration, $\mathbf{G}_B$ and $\mathbf{G}_V$ being initially set to the null matrix of size $m \times m$.

A difficulty is that we are not able to easily compute a value of $\mathbf{C}_A$ which is a solution of (12), for arbitrary values of $\mathbf{G}_B$ and $\mathbf{G}_V$. To address this question, (12) can be manipulated to obtain

$$\begin{aligned} \left(g_0\mathbf{1}_m - \mathbf{G}_V\right)\left(\mathbf{M} + \mathbf{N}\mathbf{M}^{-1}\mathbf{N}\right) &= \mathbf{G}_T + \mathbf{B}_T\mathbf{M}^{-1}\mathbf{N}, \\ \left(g_0\mathbf{1}_m - \mathbf{G}_V\right)\left(\mathbf{M}\mathbf{N}^{-1}\mathbf{M} + \mathbf{N}\right) &= \mathbf{G}_T\mathbf{N}^{-1}\mathbf{M} + \mathbf{B}_T, \\ \left(g_0\mathbf{1}_m - \mathbf{G}_V\right)\left(\left(\mathbf{M}\mathbf{N}^{-1}\right)^2 + \mathbf{1}_m\right) &= \left(\mathbf{G}_T\mathbf{N}^{-1}\mathbf{M} + \mathbf{B}_T\right)\mathbf{N}^{-1}, \end{aligned} \tag{B.1}$$

where we have assumed that $\mathbf{N}$ is invertible. Using (11), we get

$$\left(g_0\mathbf{1}_m - \mathbf{G}_V\right)\left(\left(\left(\mathbf{1}_m + \mathbf{R}\mathbf{G}_T - \omega\mathbf{L}\mathbf{B}_T\right)\mathbf{N}^{-1}\right)^2 + \mathbf{1}_m\right) = \left(\mathbf{G}_T\mathbf{N}^{-1}\mathbf{M} + \mathbf{B}_T\right)\mathbf{N}^{-1} \tag{B.2}$$

which may be manipulated to obtain

$$\left(\left(\mathbf{1}_m + \mathbf{R}\mathbf{G}_T - \omega\mathbf{L}\mathbf{B}_T\right)\mathbf{N}^{-1}\right)^2 = \left(g_0\mathbf{1}_m - \mathbf{G}_V\right)^{-1}\left(\mathbf{G}_T\mathbf{N}^{-1}\mathbf{M} + \mathbf{B}_T\right)\mathbf{N}^{-1} - \mathbf{1}_m, \tag{B.3}$$

$$\left(\mathbf{N}^{-1}\left(\mathbf{1}_m + \mathbf{R}\mathbf{G}_T - \omega\mathbf{L}\mathbf{B}_T\right)\right)^2 = \mathbf{N}^{-1}\left(g_0\mathbf{1}_m - \mathbf{G}_V\right)^{-1}\left(\mathbf{G}_T\mathbf{N}^{-1}\mathbf{M} + \mathbf{B}_T\right) - \mathbf{1}_m. \tag{B.4}$$

A possible solution of (B.4) is

$$\mathbf{1}_m + \mathbf{R}\mathbf{G}_T - \omega\mathbf{L}\mathbf{B}_T = \mp\mathbf{N}\left[\mathbf{N}^{-1}\left(g_0\mathbf{1}_m - \mathbf{G}_V\right)^{-1}\left(\mathbf{G}_T\mathbf{N}^{-1}\mathbf{M} + \mathbf{B}_T\right) - \mathbf{1}_m\right]^{1/2}. \tag{B.5}$$

Thus, a possible solution of (12) may satisfy

$$\mathbf{B}_T = \left(\omega\mathbf{L}\right)^{-1}\left(\mathbf{1}_m + \mathbf{R}\mathbf{G}_T \pm \mathbf{N}\left[\mathbf{N}^{-1}\left(g_0\mathbf{1}_m - \mathbf{G}_V\right)^{-1}\left(\mathbf{G}_T\mathbf{N}^{-1}\mathbf{M} + \mathbf{B}_T\right) - \mathbf{1}_m\right]^{1/2}\right) \tag{B.6}$$

in which, according to (11), $\mathbf{N}$ unfortunately depends on $\mathbf{B}_T$. However, it may easily be shown that, in the special case where $\mathbf{R}$ is the null matrix, using (11) we get

$$\mathbf{N}\left[\mathbf{N}^{-1}\left(g_0\mathbf{1}_m - \mathbf{G}_V\right)^{-1}\left(\mathbf{G}_T\mathbf{N}^{-1}\mathbf{M} + \mathbf{B}_T\right) - \mathbf{1}_m\right]^{1/2} = \omega\mathbf{L}\mathbf{G}_T\left[\left(\omega\mathbf{L}\left(g_0\mathbf{1}_m - \mathbf{G}_V\right)\omega\mathbf{L}\mathbf{G}_T\right)^{-1} - \mathbf{1}_m\right]^{1/2} \tag{B.7}$$

so that

$$\mathbf{B}_T = \left(\omega\mathbf{L}\right)^{-1} \pm \mathbf{G}_T\left[\left(\omega\mathbf{L}\left(g_0\mathbf{1}_m - \mathbf{G}_V\right)\omega\mathbf{L}\mathbf{G}_T\right)^{-1} - \mathbf{1}_m\right]^{1/2}. \tag{B.8}$$

Input: frequency of operation, Z_{Sant}.
Output: approximate nominal values of C_A and C_U, maximal value of the index k, and resulting $F({Z_U}^{(k)})$.
(1) compute ${C_A}^{(0)}$ as the value of C_A given by (A.3) and (C.3) in which $G_B = G_V = 0\,\text{S}$
(2) compute ${C_U}^{(0)}$ as the value of C_U given by (A.3) and (A.5) in which $G_B = 0\,\text{S}$ and $C_A = {C_A}^{(0)}$
(3) $k \leftarrow 0$
(4) compute $F({Z_U}^{(0)})$
(5) while $(k < 25) \wedge (F({Z_U}^{(k)}) > 10^{-4})$
(6) $k \leftarrow k + 1$
(7) compute ${C_A}^{(k)}$ as the value of C_A given by (A.3) and (C.3) in which $G_B = G_B({C_A}^{(k-1)})$ and $G_V = G_V({C_U}^{(k-1)})$
(8) compute ${C_U}^{(k)}$ as the value of C_U given by (A.3) and (A.5) in which $G_B = G_B({C_A}^{(k-1)})$ and $C_A = {C_A}^{(k)}$
(9) compute $F({Z_U}^{(k)})$
(10) compute the nominal value of C_A corresponding to ${C_A}^{(k)}$ at the frequency of operation
(11) compute the nominal value of C_U corresponding to ${C_U}^{(k)}$ at the frequency of operation
(12) return said nominal value of C_A, said nominal value of C_U, k and $F({Z_U}^{(k)})$

Algorithm 2: Iterative algorithm for computing approximate nominal values of C_A and C_U.

Thus, for $\mathbf{R} = \mathbf{0}\,\Omega$ the right-hand side of (B.6) does not depend on $\mathbf{B}_T$. This indicates that, for small losses in the coil, that is, for $|||\omega\mathbf{L}|||_\infty \gg |||\mathbf{R}|||_\infty$, the part of the right-hand side of (B.6) which depends on $\mathbf{B}_T$ may be treated as a small perturbation.

Thus, approximate values of $\mathbf{C}_A$, $\mathbf{G}_B$, $\mathbf{C}_U$, and $\mathbf{G}_V$ satisfying (6) can be computed using an iterative algorithm in which

(i) ${\mathbf{C}_A}^{(0)}$ is a solution of (12) obtained for $\mathbf{R} = \mathbf{0}\,\Omega$ and $\mathbf{G}_B = \mathbf{G}_V = \mathbf{0}\,\text{S}$, given by (7) and (B.8), and ${\mathbf{C}_U}^{(0)}$ is given by (7), (11), and (13) in which $\mathbf{R} = \mathbf{0}\,\Omega$, $\mathbf{G}_B = \mathbf{0}\,\text{S}$ and $\mathbf{C}_A = {\mathbf{C}_A}^{(0)}$;

(ii) for a positive integer k, ${\mathbf{C}_A}^{(k)}$ is an *approximate* solution of (12) obtained for $\mathbf{G}_B = \mathbf{G}_B({\mathbf{C}_A}^{(k-1)})$ and $\mathbf{G}_V = \mathbf{G}_V({\mathbf{C}_U}^{(k-1)})$, given by (7), (11), and (B.6) in which $\mathbf{G}_B = \mathbf{G}_B({\mathbf{C}_A}^{(k-1)})$ and $\mathbf{G}_V = \mathbf{G}_V({\mathbf{C}_U}^{(k-1)})$ and in which, except in the left-hand side of (B.6), $\mathbf{C}_A = {\mathbf{C}_A}^{(k-1)}$, and ${\mathbf{C}_U}^{(k)}$ is given by (7), (11), and (13) in which $\mathbf{G}_B = \mathbf{G}_B({\mathbf{C}_A}^{(k-1)})$ and $\mathbf{C}_A = {\mathbf{C}_A}^{(k)}$.

Appendix C shows how the iterative algorithm can be simplified in the special case $m = 1$.

C. Derivation of a Tuning Computation Technique for a SAPSUP Antenna Tuner

In the case of a π-network SAPSUP antenna tuner, the results of Appendix B may be simplified as follows. Here, (A.4) may be written

$$\begin{aligned}(g_0 - G_V)\left[1 + \left(R^2 + (\omega L)^2\right)\left(G_T^2 + B_T^2\right) + 2RG_T\right.\\ \left. - 2\omega L B_T\right] = G_T + R\left(G_T^2 + B_T^2\right).\end{aligned} \tag{C.1}$$

Thus, in an iterative algorithm at each step of which G_B and G_V are regarded as constant, (A.4) becomes the quadratic equation

$$\begin{aligned}&\left\{(g_0 - G_V)\left((\omega L)^2 + R^2\right) - R\right\} B_T^2\\ &\quad - 2\omega L\left(g_0 - G_V\right) B_T\\ &\quad + \left(g_0 - G_V\right)\left\{(1 + RG_T)^2 + (\omega L G_T)^2\right\} - G_T\\ &\quad - RG_T^2 = 0\end{aligned} \tag{C.2}$$

of unknown B_T, the solutions of which are given by

$$B_T = \frac{\omega L \pm \sqrt{(\omega L)^2 - \left[(\omega L)^2 + R^2 - \left(R/\left(g_0 - G_V\right)\right)\right] \times \left[(1 + RG_T)^2 + (\omega L G_T)^2 - \left(\left(G_T + RG_T^2\right)/\left(g_0 - G_V\right)\right)\right]}}{(\omega L)^2 + R^2 - \left(R/\left(g_0 - G_V\right)\right)}. \tag{C.3}$$

Here, approximate values C_A, G_B, C_U, and G_V satisfying (A.2) can be computed using an iterative algorithm in which

(i) ${C_A}^{(0)}$ is a solution of (A.4) obtained for $G_B = G_V = 0\,\text{S}$, given by (A.3) and (C.3) in which $G_B = G_V = 0\,\text{S}$; and ${C_U}^{(0)}$ is given by (A.3) and (A.5) in which $C_A = {C_A}^{(0)}$ and $G_B = 0\,\text{S}$;

(ii) for a positive integer k, ${C_A}^{(k)}$ is a solution of (A.4) obtained for $G_B = G_B({C_A}^{(k-1)})$ and $G_V = G_V({C_U}^{(k-1)})$, given by (A.3) and (C.3) in which $G_B = G_B({C_A}^{(k-1)})$ and $G_V = G_V({C_U}^{(k-1)})$; and ${C_U}^{(k)}$ is given by (A.3) and (A.5) in which $C_A = {C_A}^{(k)}$ and $G_B = G_B({C_A}^{(k-1)})$.

The full algorithm is shown in the box "Algorithm 2." A major difference between this algorithm and the one proposed in Section 4 and Appendix B for the MAPMUP antenna tuner is that (C.3) is an exact solution of (A.4) for known G_B and G_V, whereas no exact solution of (12) is available in Appendix B, except (B.8) for $\mathbf{R} = \mathbf{0}\,\Omega$.

At each step $k \geq 0$ in the iteration, there is no guaranty that $C_A{}^{(k)}$ and $C_U{}^{(k)}$ are real and that $C_A{}^{(k)} > 0$ and $C_U{}^{(k)} > 0$. At each step $k \geq 0$ in the iteration, we compute $F(Z_U{}^{(k)})$, where we use $Z_U{}^{(k)}$ to denote the value of Z_U given by (A.1) for $C_A = C_A{}^{(k)}$, $G_B = G_B(C_A{}^{(k)})$, $C_U = C_U{}^{(k)}$, and $G_V = G_V(C_U{}^{(k)})$ and where, for an arbitrary impedance Z, the return figure $F(Z)$ is

$$F(Z) = \left| \frac{Z - r_0}{Z + r_0} \right|. \tag{C.4}$$

that is, $F(Z)$ is the absolute value of a reflection coefficient. A sufficiently small value of $F(Z_U{}^{(k)})$ ends the iteration.

Competing Interests

The authors declare that they have no competing interests.

References

[1] N. Murtaza, M. Hein, and E. Zameshaeva, "Reconfigurable decoupling and matching network for a cognitive antenna," in *Proceedings of the 41st European Microwave Conference (EuMC '11)*, pp. 874–877, Manchester, UK, October 2011.

[2] X. Tang, K. Mouthaan, and J. C. Coetzee, "Tunable decoupling and matching network for diversity enhancement of closely spaced antennas," *IEEE Antennas and Wireless Propagation Letters*, vol. 11, pp. 268–271, 2012.

[3] A. Krewski and W. L. Schroeder, "Electrically tunable mode decomposition network for 2-port MIMO antennas," in *Proceedings of the 2013 Loughborough Antennas and Propagation Conference (LAPC '13)*, pp. 553–558, Loughborough, UK, November 2013.

[4] U.S. patent no. 9,337,534, "Method and device for radio reception using an antenna tuning apparatus and a plurality of antennas," Priority: French patent application 12/02564 of 27 September 2012.

[5] U.S. patent no. 9,077,317, "Method and apparatus for automatically tuning an impedance matrix, and radio transmitter using this apparatus". Priority: French patent application 13/00878 of 15 April 2013.

[6] I. Vasilev, V. Plicanic, and B. K. Lau, "Impact of antenna design on MIMO performance for compact terminals with adaptive impedance matching," *IEEE Transactions on Antennas and Propagation*, vol. 64, no. 4, pp. 1454–1465, 2016.

[7] W. P. Geren, C. R. Curry, and J. Andersen, "A practical technique for designing multiport coupling networks," *IEEE Transactions on Microwave Theory and Techniques*, vol. 44, no. 3, pp. 364–371, 1996.

[8] J. W. Wallace and M. A. Jensen, "Termination-dependent diversity performance of coupled antennas: network theory analysis," *IEEE Transactions on Antennas and Propagation*, vol. 52, no. 1, pp. 98–105, 2004.

[9] J. Weber, C. Volmer, K. Blau, R. Stephan, and M. A. Hein, "Miniaturisation of antenna arrays for mobile communications," in *Proceedings of the 35th European Microwave Conference*, pp. 1173–1176, Paris, France, October 2005.

[10] J. Weber, C. Volmer, K. Blau, R. Stephan, and M. A. Hein, "Miniaturized antenna arrays using decoupling networks with realistic elements," *IEEE Transactions on Microwave Theory and Techniques*, vol. 54, no. 6, pp. 2733–2740, 2006.

[11] J. Weber, C. Volmer, K. Blau, R. Stephan, and M. A. Hein, "Implementation of a miniaturized antenna array with predefined orthogonal radiation patterns," in *Proceedings of the European Conference on Antennas and Propagation (EuCAP '06)*, pp. 1–5, Nice, France, November 2006.

[12] A. Krewski, W. L. Schroeder, and K. Solbach, "Matching network synthesis for mobile MIMO antennas based on minimization of the total multi-port reflectance," in *Proceedings of the 7th Loughborough Antennas and Propagation Conference (LAPC '11)*, pp. 1–4, Loughborough, UK, November 2011.

[13] A. Krewski and W. L. Schroeder, "N-port DL-MIMO antenna system realization using systematically designed mode matching and mode decomposition network," in *Proceedings of the 2012 42nd European Microwave Conference (EuMC '12)-Held as Part of 15th European Microwave Week (EuMW '12)*, pp. 156–159, Amsterdam, Netherlands, November 2012.

[14] F. Broydé and E. Clavelier, "Some properties of multiple-antenna-port and multiple-user-port antenna tuners," *IEEE Transactions on Circuits and Systems I: Regular Papers*, vol. 62, no. 2, pp. 423–432, 2015.

[15] F. Broydé and E. Clavelier, "A new multiple-antenna-port and multiple-user-port antenna tuner," in *Proceedings of the IEEE Radio & Wireless Week (RWW '15)*, pp. 41–43, San Diego, Calif, USA, January 2015.

[16] F. Broydé and E. Clavelier, "Two multiple-antenna-port and multiple-user-port antenna tuners," in *Proceedings of the 9th European Conference on Antennas and Propagation (EuCAP '15)*, Lisbon, Portugal, April 2015.

[17] R. A. Horn and C. R. Johnson, *Matrix Analysis*, Cambridge University Press, Cambridge, UK, 2nd edition, 2013.

[18] R. A. Horn and C. R. Johnson, *Topics in Matrix Analysis*, Cambridge University Press, Cambridge, UK, 1991.

[19] *The A. R. R. L. Antenna Book*, The American Radio Relay League, 8th edition, 1956.

[20] R. G. Vaughan and J. B. Andersen, "Antenna diversity in mobile communications," *IEEE Transactions on Vehicular Technology*, vol. 36, no. 4, pp. 149–172, 1987.

[21] S. Stein, "On cross coupling in multiple-beam antennas," *IRE Transactions on Antennas and Propagation*, vol. 10, no. 5, pp. 548–557, 1962.

[22] K. Wang, L. Li, and T. F. Eibert, "Estimation of signal correlation of lossy compact monopole arrays with decoupling networks," *IEEE Transactions on Antennas and Propagation*, vol. 63, no. 1, pp. 357–363, 2015.

[23] W.-K. Chen, Ed., *The Circuits and Filters Handbook*, CRC Press/IEEE Press, 1995.

[24] US patent no. 5,564,086, "Method and apparatus for enhancing an operating characteristic of a radio transmitter," Filed: November 29, 1993.

[25] U.S. patent no. 6,414,562, "Circuit and method for impedance matching," Filed: May 27, 1997.

[26] International application no. PCT/IB2015/057161, "Method for automatically adjusting a tuning unit, and automatic tuning system using this method," Priority: French patent application 15/01780 of 26 August 2015.

[27] Y. Sun and J. K. Fidler, "Design of Π impedance matching networks," in *Proceedings of the IEEE International Symposium on Circuits and Systems*, vol. 5, pp. 5–8, London, UK, June 1994.

[28] Q. Gu, J. R. De Luis, I. Morris, and J. Hilbert, "An analytical algorithm for pi-network impedance tuners," *IEEE Transactions on Circuits and Systems I. Regular Papers*, vol. 58, no. 12, pp. 2894–2905, 2011.

About the Beam Cosines and the Radiation Efficiency of a Multiport Antenna Array

Frédéric Broydé, Evelyne Clavelier
Excem, Maule, France (emails: fredbroyde@eurexcem.com, eclavelier@eurexcem.com)

***Abstract* — The paper establishes some properties of the matrix of the beam cosines of the radiated power of a multiport antenna array (MAA), and of the matrix of the beam cosines of the delivered power, which concerns reception by the MAA. These matrices are related to several quantities used in the literature. Though these matrices are usually different and complex, the paper explains why they may be equal and real, under certain assumptions. The paper also proposes a definition and an investigation of the radiation efficiency of the MAA.**

***Index Terms* — Antenna theory, multiport antenna arrays, MIMO radio communication.**

I. Introduction

We consider a multiport antenna array (MAA) having m ports numbered from 1 to m, where $m \geq 2$. The MAA may for instance only comprise m antennas, as shown in Fig. 1(A). It may also include a multiple-antenna-port and multiple-user-port (MAPMUP) antenna tuner [1]-[6] and/or one or more feeders, in addition to the antennas, as shown in Fig. 1(B). We assume that the MAA is linear, but we do not assume reciprocity.

In analytic geometry, direction cosine refers to the cosine of the angle between two vectors $\mathbf{v}_1$ and $\mathbf{v}_2$, that is the quantity $\mathbf{v}_1 \cdot \mathbf{v}_2 /(\|\mathbf{v}_1\| \, \|\mathbf{v}_2\|)$. By analogy, in this paper, some quantities in the form $<\psi_1, \psi_2>/(<\psi_1, \psi_1><\psi_2, \psi_2>)^{1/2}$, where the brackets denote an hermitian product involving an integration over all directions in space, are called "beam cosines" [7, ch. 12].

In [6], we computed several beam cosines of an MAA comprising a MAPMUP antenna tuner. However, we did not explain some visible characteristics of their computed values, and, to our best knowledge, the literature does not help to understand them. This paper provides a new analysis of the properties of the beam cosines, in § II and § III. The paper also proposes a new definition of the radiation efficiency of the MAA, and derives some of its attributes in § IV.

II. Beam Cosines of the Radiated Power

We will use a spherical coordinate system having an origin somewhere close to the MAA, θ being the zenithal angle (i.e. the angle with respect to the z-axis) and φ being the azimuth angle. In this § II, the MAA is used for emission. A linear multiport source (LMS) has m ports numbered from 1 to m. Its admittance matrix is denoted by $\mathbf{Y}_S$. We do not assume that $\mathbf{Y}_S$ is diagonal. For any $\alpha \in \{1,..., m\}$, port α of the MAA is coupled to port α of the LMS.

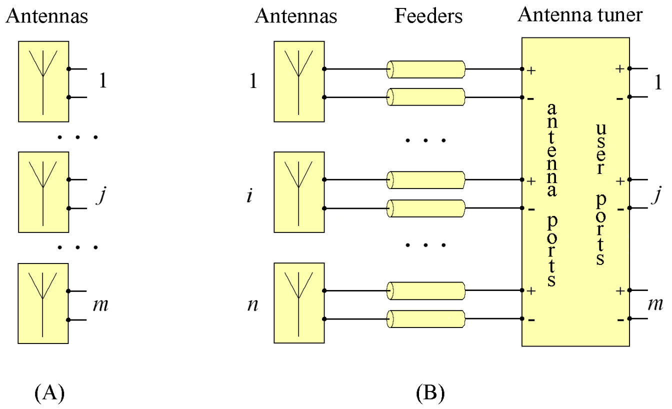

Fig. 1. An MAA consisting of m antennas in (A), and an MAA consisting of n antennas, their feeders and a MAPMUP antenna tuner having n antenna ports and m user ports (B).

Let $\mathbf{I}_0$ be the $m \times 1$ column vector of the rms short-circuit currents at the ports of the LMS. For $\alpha \in \{1,..., m\}$, let $\mathbf{I}_{0\,\alpha}$ be a particular value of $\mathbf{I}_0$ having all its entries equal to zero ampere, except the entry of the row α, which takes on a specified value I_α. For $\alpha \in \{1,..., m\}$, let $\mathbf{E}_{0\,\alpha}$ be the electric field radiated by the MAA in a configuration where $\mathbf{I}_0$ is equal to $\mathbf{I}_{0\,\alpha}$. Clearly, $\mathbf{E}_{0\,\alpha}$ is proportional to I_α. A plot of the average radiation intensity of $\mathbf{E}_{0\,\alpha}$ in the far field, as a function of an angle, may be referred to as a radiation pattern of port α.

Let $\mathbf{P}_R$ be the matrix of the self- and cross complex powers radiated by the MAA over all values of θ and φ, defined as follows: for $\alpha \in \{1,..., m\}$ and $\beta \in \{1,..., m\}$, the entry $P_{R\,\alpha\beta}$ of $\mathbf{P}_R$ is given by

$$P_{R\alpha\beta} = \frac{1}{\eta_0} \int_0^{\pi} \int_0^{2\pi} \mathbf{E}_{0\alpha}^{*} \mathbf{E}_{0\beta} \, r^2 \sin\theta \; d\varphi \, d\theta \qquad (1)$$

where $\eta_0 \approx 376.7\ \Omega$ is the intrinsic impedance of free space, where $\mathbf{E}_{0\,\alpha}$ and $\mathbf{E}_{0\,\beta}$ are regarded as column vectors, where the star denotes the Hermitian adjoint, and where the integration is carried out at a large distance r from the antennas lying in free space. Clearly, $P_{R\,\alpha\beta}$ is proportional to $\overline{I_\alpha}$ and to I_β, where the bar indicates the complex conjugate.

For $\alpha \in \{1,..., m\}$, since $\mathbf{E}_{0\,\alpha}$ is caused by the short-circuit current I_α of the port α of the LMS, we can consider that $\mathbf{E}_{0\,\alpha}$ is the electric field produced by a single-port antenna made up of the MAA and a linear passive multiport circuit (PMC) having m ports numbered from 1 to m, of admittance matrix $\mathbf{Y}_S$, each port of the PMC being coupled to the port of same number of the MAA, the port of the single-port antenna being port α of the

Proceedings of the12th European Conference on Antennas and Propagation, EuCAP 2018, April 2018.

MAA coupled to port α of the PMC, this single-port antenna being coupled to a single-port current source delivering I_α. Let $\mathbf{h}_{0\,\alpha}$ be the effective complex length of this single-port antenna in a direction (θ, φ), as defined in [8, § 5.2]. We have

$$\mathbf{E}_{0\alpha} = j\eta_0 \frac{I_\alpha\, k\, e^{-jkr}}{4\pi\, r}\, \mathbf{h}_{0\alpha} \tag{2}$$

where k is the wave number. Consequently, we have

$$P_{R\alpha\beta} = \frac{\eta_0 k^2 \overline{I_\alpha} I_\beta}{16\pi^2} \int_0^{\pi} \int_0^{2\pi} \mathbf{h}_{0\alpha}^* \mathbf{h}_{0\beta} \sin\theta \; d\varphi\, d\theta \tag{3}$$

Since, for any $\alpha \in \{1,..., m\}$ and any $\beta \in \{1,..., m\}$, by (1), $P_{R\alpha\beta}$ is an hermitian product (or inner product) of the beams $\mathbf{E}_{0\beta}$ and $\mathbf{E}_{0\,\alpha}$, we can, if $P_{R\,\alpha\,\alpha} \neq 0$ and $P_{R\,\beta\,\beta} \neq 0$, define the beam cosines of the radiated power, denoted by $\rho_{R\,\alpha\,\beta}$ and given by

$$\rho_{R\alpha\beta} = \frac{P_{R\alpha\beta}}{\sqrt{P_{R\alpha\alpha} P_{R\beta\beta}}} \tag{4}$$

The matrix $(\rho_{R\,\alpha\,\beta})$ is Hermitian. Note that $|\rho_{R\,\alpha\,\beta}|$ is sometimes referred to as "orthogonality coefficients", for instance in [9]. Also, $|\,\rho_{R\,\alpha\,\beta}\,|^2$ is related to the "envelope correlation" considered in [10] and to the "correlation coefficient" considered in [11, pp. 248-249]. We note that $\rho_{R\,\alpha\,\beta}$ may exist only if $I_\alpha \neq 0$ and $I_\beta \neq 0$, that $\rho_{R\,\alpha\,\beta}$ is proportional to $\overline{I_\alpha}/|I_\alpha|$ and to $I_\beta/|I_\beta|$, and that $|\,\rho_{R\,\alpha\,\beta}\,|$ and $|\,\rho_{R\,\alpha\,\beta}\,|^2$ are independent of I_α and I_β.

For an arbitrary $\mathbf{I}_0$, let $\mathbf{E}_0$ be the electric field radiated by the MAA and let P_{rad} be the average power radiated by the MAA. For any $\alpha \in \{1,..., m\}$, we now use I_α to denote the entry of the row α of $\mathbf{I}_0$. P_{rad} is given by

$$P_{\text{rad}} = \frac{1}{\eta_0} \int_0^{\pi} \int_0^{2\pi} \mathbf{E}_0^* \mathbf{E}_0\, r^2 \sin\theta \; d\varphi\, d\theta \tag{5}$$

where $\mathbf{E}_0$ is regarded as a column vector, and where the integration is carried out at a large distance r from the antennas lying in free space. By superposition, we have

$$\mathbf{E}_0 = \sum_{\alpha=1}^{m} \mathbf{E}_{0\alpha} = j\eta_0 \frac{k\, e^{-jkr}}{4\pi\, r} \sum_{\alpha=1}^{m} I_\alpha\; \mathbf{h}_{0\alpha} \tag{6}$$

so that

$$P_{\text{rad}} = \frac{\eta_0 k^2}{16\pi^2} \sum_{\alpha=1}^{m} \sum_{\beta=1}^{m} \overline{I_\alpha} I_\beta \int_0^{\pi} \int_0^{2\pi} \mathbf{h}_{0\alpha}^* \mathbf{h}_{0\beta} \sin\theta \; d\varphi\, d\theta \tag{7}$$

Let $\mathbf{Z}_{\text{rad}}$ be the matrix such that, for any $\alpha \in \{1,..., m\}$ and any $\beta \in \{1,..., m\}$, the entry of the row α and the column β of $\mathbf{Z}_{\text{rad}}$, denoted by $Z_{\text{rad}\,\alpha\,\beta}$, is given by

$$Z_{\text{rad}\alpha\beta} = \frac{\eta_0 k^2}{16\pi^2} \int_0^{\pi} \int_0^{2\pi} \mathbf{h}_{0\alpha}^* \mathbf{h}_{0\beta} \sin\theta \; d\varphi\, d\theta \tag{8}$$

We see that $\mathbf{Z}_{\text{rad}}$ is an Hermitian matrix, that it has the dimensions of impedance, and that

$$P_{\text{rad}} = \mathbf{I}_0^*\, \mathbf{Z}_{\text{rad}}\, \mathbf{I}_0 \tag{9}$$

Thus, P_{rad} is an Hermitian quadratic form of the variable $\mathbf{I}_0$, and $\mathbf{Z}_{\text{rad}}$ is the only matrix which satisfies (9) for any value of $\mathbf{I}_0$ [12, § 3.2.4], [13, p. 174 Problem 6]. Moreover, since $P_{\text{rad}} \geq 0$ for any value of $\mathbf{I}_0$, it follows that $\mathbf{Z}_{\text{rad}}$ is positive semidefinite.

If we use $\mathbf{Y}_A$ to denote the admittance matrix presented by the MAA, we find that the average power received by the ports of the MAA, denoted by P_{ANT}, is given by

$$P_{\text{ANT}} = \mathbf{I}_0^*\, \mathbf{Z}_{\text{pow}}\, \mathbf{I}_0 \tag{10}$$

where

$$\mathbf{Z}_{\text{pow}} = \left(\mathbf{Y}_A + \mathbf{Y}_S\right)^{-1*} \frac{\mathbf{Y}_A + \mathbf{Y}_A^*}{2} \left(\mathbf{Y}_A + \mathbf{Y}_S\right)^{-1} \tag{11}$$

is an impedance matrix, and Hermitian. Since $P_{\text{ANT}} \geq 0$ for any value of $\mathbf{I}_0$, it follows that $\mathbf{Z}_{\text{pow}}$ is positive semidefinite. In the special case where $\mathbf{Y}_A$ is symmetric (reciprocal MAA), the ratio $(\mathbf{Y}_A + \mathbf{Y}_A{}^*)/2$ is the real part of $\mathbf{Y}_A$.

It follows from the conservation of average power that we have

$$P_{\text{ANT}} = P_{\text{rad}} + P_{\text{loss}} \tag{12}$$

where P_{loss} is the loss in the MAA. Using (9), (10) and (12), we find that

$$P_{\text{loss}} = \mathbf{I}_0^*\, \mathbf{Z}_{\text{loss}}\, \mathbf{I}_0 \tag{13}$$

where

$$\mathbf{Z}_{\text{loss}} = \mathbf{Z}_{\text{pow}} - \mathbf{Z}_{\text{rad}} \tag{14}$$

is an impedance matrix, which is Hermitian. We see that P_{loss} is an Hermitian quadratic form of the variable $\mathbf{I}_0$, so that $\mathbf{Z}_{\text{loss}}$ is the only matrix which satisfies (13) for any value of $\mathbf{I}_0$. Since $P_{\text{loss}} \geq 0$ for any value of $\mathbf{I}_0$, $\mathbf{Z}_{\text{loss}}$ is positive semidefinite.

For any $\alpha \in \{1,..., m\}$ and any $\beta \in \{1,..., m\}$, let $Z_{\text{pow}\,\alpha\,\beta}$ and $Z_{\text{loss}\,\alpha\,\beta}$ be the entries of the row α and the column β of $\mathbf{Z}_{\text{pow}}$ and $\mathbf{Z}_{\text{loss}}$, respectively. By (8) and (14), we have

$$Z_{\text{pow}\alpha\beta} - Z_{\text{loss}\alpha\beta} = \frac{\eta_0 k^2}{16\pi^2} \int_0^{\pi} \int_0^{2\pi} \mathbf{h}_{0\alpha}^* \mathbf{h}_{0\beta} \sin\theta \; d\varphi\, d\theta \tag{15}$$

Using (3), we obtain

$$P_{R\alpha\beta} = \left(Z_{\text{pow}\alpha\beta} - Z_{\text{loss}\alpha\beta}\right) \overline{I_\alpha} I_\beta \tag{16}$$

so that, using (4) we get

$$\rho_{R\alpha\beta} = \frac{Z_{\text{pow}\alpha\beta} - Z_{\text{loss}\alpha\beta}}{\sqrt{\left(Z_{\text{pow}\alpha\alpha} - Z_{\text{loss}\alpha\alpha}\right)\left(Z_{\text{pow}\beta\beta} - Z_{\text{loss}\beta\beta}\right)}} \frac{\overline{I_\alpha}}{|I_\alpha|} \frac{I_\beta}{|I_\beta|} \tag{17}$$

Formula (17) is similar to, but more general than formula (4) of [9] about $|\rho_{R\,\alpha\,\beta}|$. The main application of this formula is in the case where losses are negligible, for which

$$\rho_{R\alpha\beta} \approx \frac{Z_{\text{pow}\alpha\beta}}{\sqrt{Z_{\text{pow}\alpha\alpha} Z_{\text{pow}\beta\beta}}} \frac{\overline{I_\alpha}}{|I_\alpha|} \frac{I_\beta}{|I_\beta|} \tag{18}$$

so that, in this case, using (11), the beam cosines can be derived from $\mathbf{Y}_S$ and a measurement of $\mathbf{Y}_A$. Formula (18) is similar to, but more general than the result obtained in [10] about $|\rho_{R\,\alpha\,\beta}|$. It entails that, if $\mathbf{Y}_S$ and $\mathbf{Y}_A$ are diagonal, then the beams are orthogonal (an old result [14]), since in this case, for $\alpha \neq \beta$, we have $Z_{\text{pow}\,\alpha\beta} = 0\ \Omega$ so that $\rho_{R\,\alpha\beta} \approx 0$. The orthogonality considered here is "over all directions in space", as opposed to an orthogonality "over the azimuth φ" which does not seem to exist.

Beam cosines of the radiated power were computed in [6, § 6] for an MAA composed of 4 antennas, 4 feeders and a lossy MAPMUP antenna tuner having 4 antenna ports and 4 user ports. At 800 MHz, radiation patterns of the ports of the MMA are shown in Fig. 2, and the matrix of the beam cosines of the radiated power is approximately given by

$$\left(\rho_{R\alpha\beta}\right) \approx \begin{pmatrix} 1.000 & 0.308 & -0.029 & 0.308 \\ 0.308 & 1.000 & 0.308 & -0.029 \\ -0.029 & 0.308 & 1.000 & 0.308 \\ 0.308 & -0.029 & 0.308 & 1.000 \end{pmatrix} \tag{19}$$

We observe that this matrix is real. This is caused by the particular configuration of the antennas, feeders and antenna tuner, and by the choice of the relative phases of $I_1, \ldots, I_m$. More precisely, let us assume that the electrical and electromagnetic properties of the antennas are invariant under the symmetries of the point group denoted by $C_{m\,v}$ in the Schönflies notation [15, ch. 2], each of these symmetries being associated with an appropriate permutation of the ports of the MAA, and of the internal connections of the MAA. The point group $C_{m\,v}$ contains m rotations of angle $2\pi p/m$ about an axis, where $p \in \{0,\ldots, m-1\}$, and m reflections in planes containing the axis. Without loss of generality, we may assume that this axis is the z-axis of the spherical coordinate system. For given α and β, the permutation associated with one of the reflection planes transforms port α into port β, and port β into port α. Without loss of generality, we may assume that this reflection plane contains the x-axis of the spherical coordinate system, so that a reflection by this plane transforms a direction (θ, φ) into a direction $(\theta, -\varphi)$. If we apply $\mathbf{I}_{0\,\alpha}$, we may use $\mathbf{h}_{0\,\alpha}(\theta, \varphi)$ and $\mathbf{h}_{0\,\alpha}(\theta, -\varphi)$ to denote the values of $\mathbf{h}_{0\alpha}$ in the directions (θ, φ) and $(\theta, -\varphi)$, respectively. If we apply $\mathbf{I}_{0\,\beta}$, we may use $\mathbf{h}_{0\,\beta}(\theta, \varphi)$ and $\mathbf{h}_{0\,\beta}(\theta, -\varphi)$ to denote the values of $\mathbf{h}_{0\beta}$ in the directions (θ, φ) and $(\theta, -\varphi)$, respectively. If $\mathbf{Y}_S$ is invariant under the associated permutation of the ports, we may conclude that $\mathbf{h}_{0\,\alpha}(\theta, \varphi) = \mathbf{h}_{0\,\beta}(\theta, -\varphi)$, and also that $\mathbf{h}_{0\,\alpha}(\theta, -\varphi) = \mathbf{h}_{0\,\beta}(\theta, \varphi)$. Thus, we have

$$\begin{aligned} &\mathbf{h}^*_{0\alpha}(\theta,\varphi)\mathbf{h}_{0\beta}(\theta,\varphi) + \mathbf{h}^*_{0\alpha}(\theta,-\varphi)\mathbf{h}_{0\beta}(\theta,-\varphi) \\ &\quad = \mathbf{h}^*_{0\alpha}(\theta,\varphi)\mathbf{h}_{0\beta}(\theta,\varphi) + \mathbf{h}^*_{0\beta}(\theta,\varphi)\mathbf{h}_{0\alpha}(\theta,\varphi) \\ &\quad = 2\,\mathrm{Re}\left(\mathbf{h}^*_{0\alpha}(\theta,\varphi)\mathbf{h}_{0\beta}(\theta,\varphi)\right) \end{aligned} \tag{20}$$

where Re denotes the real part. Thus, using (3), if $I_\alpha = I_\beta$, we obtain

$$\begin{aligned} P_{R\alpha\beta} &= \frac{\eta_0 k^2 |I_\alpha|^2}{8\pi^2} \\ &\times \int_0^\pi \int_0^\pi \mathrm{Re}\left(\mathbf{h}^*_{0\alpha}(\theta,\varphi)\mathbf{h}_{0\beta}(\theta,\varphi)\right)\sin\theta \; d\phi\, d\theta \end{aligned} \tag{21}$$

so that $P_{R\,\alpha\beta}$ is real. Consequently, the matrix of the beam cosines is also real.

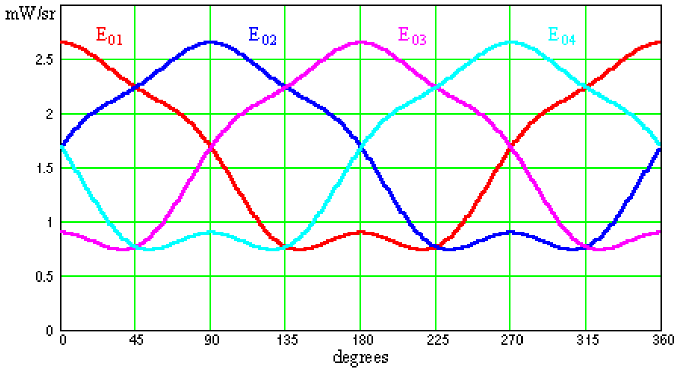

Fig. 2. Radiation patterns of the ports of the MMA, at 800 MHz, in the plane $\theta = \pi/2$, versus the azimuth angle φ, each curve corresponding to an open-circuit voltage of 2 V applied to one of the user ports of the antenna tuner.

This is what happens in [6, § 6], where the MAA is invariant under the symmetries of the point group $C_{4\,v}$ and the associated permutations. We note that the obscure explanation provided in [16] after equation (35) does not work here because the radiation patterns of the ports are not "identical patterns which are circularly symmetric", as shown in Fig. 2.

In a different configuration, the beam cosines of the radiated power need not be real.

III. Beam Cosines of the Delivered Power

Let us now consider that the MAA is used for reception. A linear multiport load (LML) has m ports numbered from 1 to m. Its admittance matrix is $\mathbf{Y}_S$. For any $\alpha \in \{1,\ldots, m\}$, port α of the MAA is coupled to port α of the LML. In a configuration where a plane wave of electric field amplitude 1 V/m rms impinges on the MAA from the direction (θ, φ), with a specified polarization which depends on (θ, φ), for any $\alpha \in \{1,\ldots, m\}$ let V_α be the rms voltage across port α of the MAA, and let $\mathbf{V}$ be the $m \times 1$ column vector of V_1 to V_m. Let g_0 be an arbitrary conductance. A plot of the power $|V_\alpha|^2/g_0$, as a function of an angle, may be referred to as a reception pattern of port α.

We assume a reciprocal MAA. We also assume a reciprocal multiport load, so that $\mathbf{Y}_S$ is symmetric. For $\alpha \in \{1,\ldots, m\}$, V_α is the open-circuit voltage of the single-port antenna defined above in § II, in the discussion of $\mathbf{E}_{0\,\alpha}$. Since $\mathbf{h}_{0\,\alpha}$ is the effective complex length of this single-port antenna in the direction (θ, φ), and using the assumed reciprocity, we have

$$V_\alpha = \mathbf{h}_{0\alpha} \cdot \mathbf{E}_{i0} \tag{22}$$

where $\mathbf{E}_{i\,0}$ is the incident electric field at the origin of the coordinate system [8, § 5.2]. Thus, if the polarization of the incident field is matched to the polarization of the single-port antenna, that is to say for $\mathbf{E}_{i\,0}$ equal to a complex constant times the complex conjugate of $\mathbf{h}_{0\,\alpha}$ [8, § 5.2] [12, § 3.3.2], we get

$$|V_\alpha| = \|\mathbf{h}_{0\alpha}\|\,\|\mathbf{E}_{i0}\| = \sqrt{\mathbf{h}_{0\alpha} \cdot \overline{\mathbf{h}_{0\alpha}}}\,\sqrt{\mathbf{E}_{i0} \cdot \overline{\mathbf{E}_{i0}}} \tag{23}$$

so that the reception pattern of port α of the MAA clearly corresponds to the directivity pattern of the single-port antenna, hence to the radiation pattern of port α of the MAA.

Let $\mathbf{P}_D$ be the matrix of the self- and cross complex powers delivered by the ports of the MAA, averaged over all directions of arrival of a plane wave of electric field amplitude 1 V/m rms impinging on the MAA with a specified polarization depending on (θ, φ), defined as follows:

$$\mathbf{P}_D = \frac{1}{4\pi}\int_0^{\pi}\int_0^{2\pi} \mathbf{V}\,\mathbf{I}^* \sin\theta \; d\varphi\, d\theta \tag{24}$$

where $\mathbf{I}$ is the $m \times 1$ column vector of the rms current flowing out of the m ports of the MAA. In (24), $\mathbf{V}$ depends on (θ, φ) according to (22), so that $\mathbf{I}$ also depends on (θ, φ). We have

$$\mathbf{P}_D = \frac{1}{4\pi}\int_0^{\pi}\int_0^{2\pi} \mathbf{V}\,\mathbf{V}^*\mathbf{Y}_S^* \sin\theta \; d\varphi\, d\theta \tag{25}$$

Let P_{del} be the average power delivered by the ports of the MAA, averaged over all directions of arrival of a plane wave of electric field amplitude 1 V/m rms impinging on the MAA with the specified polarization. We have

$$P_{\text{del}} = \frac{1}{4\pi}\int_0^{\pi}\int_0^{2\pi} \mathbf{V}^* \frac{\mathbf{Y}_S + \mathbf{Y}_S^*}{2}\mathbf{V} \sin\theta \; d\varphi\, d\theta \tag{26}$$

In the special case where $\mathbf{Y}_S = g_0\ \mathbf{1}_m$ and where $\mathbf{1}_m$ is the identity matrix of size m by m, we get

$$\mathbf{P}_D = \frac{g_0}{4\pi}\int_0^{\pi}\int_0^{2\pi} \mathbf{V}\,\mathbf{V}_0^* \sin\theta \; d\varphi\, d\theta \tag{27}$$

so that, for $\alpha \in \{1,..., m\}$ and $\beta \in \{1,..., m\}$, the entry $P_{D\alpha\beta}$ of $\mathbf{P}_D$ is given by

$$P_{D\alpha\beta} = \frac{g_0}{4\pi}\int_0^{\pi}\int_0^{2\pi} V_\alpha \overline{V_\beta} \sin\theta \; d\varphi\, d\theta \tag{28}$$

Using (22), we obtain in this special case

$$P_{D\alpha\beta} = \frac{g_0}{4\pi}\int_0^{\pi}\int_0^{2\pi} \left(\mathbf{h}_{0\alpha}\cdot\mathbf{E}_{i0}\right)\left(\overline{\mathbf{h}_{0\beta}\cdot\mathbf{E}_{i0}}\right) \sin\theta \; d\varphi\, d\theta \tag{29}$$

which is, in general, quite different from $P_{R\alpha\beta}$ given by (3). In this special case, we also have

$$P_{\text{del}} = \frac{g_0}{4\pi}\int_0^{\pi}\int_0^{2\pi} \mathbf{V}^*\mathbf{V} \sin\theta \; d\varphi\, d\theta = \operatorname{tr}\mathbf{P}_D \tag{30}$$

where tr $\mathbf{P}_D$ stands for the trace of $\mathbf{P}_D$.

Since, for any $\alpha \in \{1,..., m\}$ and any $\beta \in \{1,..., m\}$, by (28), $P_{D\alpha\beta}$ is an hermitian product of the beams V_α and V_β, we can, in the special case where $\mathbf{Y}_S = g_0\ \mathbf{1}_m$, define the beam cosines of the delivered power, denoted by $\rho_{D\alpha\beta}$ and given by

$$\rho_{D\alpha\beta} = \frac{P_{D\alpha\beta}}{\sqrt{P_{D\alpha\alpha}P_{D\beta\beta}}} \tag{31}$$

The matrix ($\rho_{D\alpha\beta}$) is Hermitian. Its entries are remotely related to the correlation coefficients discussed in [16, § III].

Beam cosines of the delivered power were computed in [6, § 6] for the same MAA and the same $\mathbf{Y}_S = 20\,\text{mS} \times \mathbf{1}_4$ as in the computation of the beam cosines of the radiated power mentioned above in § II. At 800 MHz, the matrix of the beam cosines of the delivered power is approximately given by

$$\left(\rho_{D\alpha\beta}\right) \approx \begin{pmatrix} 1.000 & 0.308 & -0.029 & 0.308 \\ 0.308 & 1.000 & 0.308 & -0.029 \\ -0.029 & 0.308 & 1.000 & 0.308 \\ 0.308 & -0.029 & 0.308 & 1.000 \end{pmatrix} \tag{32}$$

We observe that the right-hand sides of (19) and (32) are equal. To explain this, we note that each antenna had the same vertical polarization, so that $\mathbf{h}_{0\alpha}$ was collinear to the unit vector $\mathbf{e}_\theta$ of the spherical coordinate, and the polarization of the incident wave was matched because $\mathbf{E}_{i0}$ was in the form $\mathbf{E}_{i0} = E_{i0}\,\mathbf{e}_\theta$, the coordinate E_{i0} being real, so that (29) became

$$P_{D\alpha\beta} = \frac{g_0\left|E_{i0}\right|^2}{4\pi}\int_0^{\pi}\int_0^{2\pi} h_{0\alpha}\overline{h_{0\beta}} \sin\theta \; d\varphi\, d\theta \tag{33}$$

where $|E_{i0}| = 1$ V/m, and where $h_{0\alpha}$ and $h_{0\beta}$ are defined by $\mathbf{h}_{0\alpha} = h_{0\alpha}\,\mathbf{e}_\theta$ and $\mathbf{h}_{0\beta} = h_{0\beta}\,\mathbf{e}_\theta$. Moreover, since $I_\alpha = I_\beta$, (3) became

$$P_{R\alpha\beta} = \frac{\eta_0 k^2\left|I_\alpha\right|^2}{16\pi^2}\int_0^{\pi}\int_0^{2\pi} \overline{h_{0\alpha}}\, h_{0\beta} \sin\theta \; d\varphi\, d\theta \tag{34}$$

where $|I_\alpha| = 40$ mA. $P_{R\alpha\beta}$ being real for the reasons explained in § II, we have $P_{R\alpha\beta} = P_{R\beta\alpha}$. As a consequence, in the particular configuration and for the assumptions used in [6, § 6], the matrix of the beam cosines of the radiated power is equal to the matrix of the beam cosines of the delivered power.

IV. Radiation Efficiency of the MAA

Some authors consider that the radiation efficiency of a port of an MAA can be defined as the ratio of the total radiated power to the maximum power available from a single port source connected to the port, the one or more other ports of the MAA being connected to a specified multiport load [17]. This is not a good choice because:

- the radiation efficiency is originally defined, for a single port antenna, as the ratio of the total radiated power to the net power accepted by the single antenna port (that is, the power received by the single antenna port, as opposed to a forward power delivered by the source connected to it) [18, p. 30];
- a configuration in which a single port source is connected to a port of an MAA, the one or more other ports of the MAA being connected to a specified multiport load, does not represent the intended use of a typical MAA.

We define the radiation efficiency of the MAA, denoted by e, as the ratio of the total radiated power to the power received by the ports of the MAA, that is

$$e = \frac{P_{\text{rad}}}{P_{\text{ANT}}} \tag{35}$$

where we use the notations of § II and assume that $P_{\text{ANT}} \neq 0$ W. We get

$$e = \frac{\mathbf{I}_0^*\,\mathbf{Z}_{\text{rad}}\,\mathbf{I}_0}{\mathbf{I}_0^*\,\mathbf{Z}_{\text{pow}}\,\mathbf{I}_0} \tag{36}$$

where we have assumed that the denominator is nonzero. In (36), e is a function of the complex nonzero vector $\mathbf{I}_0$. Thus, e

depends on the excitation. Moreover, e is real and $e \geq 0$. Power conservation entails $e \leq 1$, so that we have $0 \leq e \leq 1$.

Let $\mathbf{A}$ be a positive definite matrix. We know that [13, § 7.2] there exists a unique positive definite matrix $\mathbf{B}$ such that $\mathbf{B}^2 = \mathbf{A}$. The matrix $\mathbf{B}$ is referred to as the unique positive definite square root of $\mathbf{A}$, and is denoted by $\mathbf{A}^{1/2}$. It satisfies $(\mathbf{A}^{1/2})^{-1} = (\mathbf{A}^{-1})^{1/2}$, and we write $\mathbf{A}^{-1/2} = (\mathbf{A}^{1/2})^{-1} = (\mathbf{A}^{-1})^{1/2}$. $\mathbf{Z}_{\text{pow}}$ is positive semidefinite as explained above in § 4.1. Assuming that $\mathbf{Z}_{\text{pow}}$ is positive definite, we can introduce the new variable $\mathbf{x} = \mathbf{Z}_{\text{pow}}{}^{1/2}\, \mathbf{I}_0$. Since $\mathbf{I}_0 = \mathbf{Z}_{\text{pow}}{}^{-1/2}\, \mathbf{x}$, we have

$$e = \left(\frac{\mathbf{x}^* \mathbf{M}\, \mathbf{x}}{\mathbf{x}^* \mathbf{x}} \right)_{\mathbf{x} \neq \mathbf{0}} \tag{37}$$

where

$$\mathbf{M} = \mathbf{Z}_{\text{pow}}^{-1/2}\, \mathbf{Z}_{\text{rad}}\, \mathbf{Z}_{\text{pow}}^{-1/2} \tag{38}$$

The matrix $\mathbf{M}$ is clearly Hermitian. Since $e \geq 0$, $\mathbf{M}$ is positive semidefinite. Let us use $\lambda_1,..., \lambda_m$ to denote the eigenvalues of $\mathbf{M}$, counting multiplicity, which are real, these eigenvalues being labeled in ascending order. By the Rayleigh-Ritz theorem [13, § 4.2] and (37), we have

$$0 \leq \lambda_1 = \min_{\mathbf{x} \neq 0} \left(\frac{\mathbf{x}^* \mathbf{M}\, \mathbf{x}}{\mathbf{x}^* \mathbf{x}} \right) \leq e \leq \lambda_m = \max_{\mathbf{x} \neq 0} \left(\frac{\mathbf{x}^* \mathbf{M}\, \mathbf{x}}{\mathbf{x}^* \mathbf{x}} \right) \leq 1 \tag{39}$$

Consequently, we have found that, if $\mathbf{Z}_{\text{pow}}$ is positive definite, λ_1 and λ_m are the minimum value and the maximum value of e, respectively, when $\mathbf{I}_0$ takes on any possible nonzero value. At this stage, to obtain λ_1 and λ_m, we need to compute $\mathbf{M}$ using (38), and then to compute its eigenvalues. The computation can be simplified significantly if we observe that

$$\mathbf{Z}_{\text{rad}}\, \mathbf{Z}_{\text{pow}}^{-1} = \mathbf{Z}_{\text{pow}}^{1/2}\, \mathbf{M}\, \mathbf{Z}_{\text{pow}}^{-1/2} \tag{40}$$

so that $\mathbf{M}$ is similar to $\mathbf{Z}_{\text{rad}}\, \mathbf{Z}_{\text{pow}}{}^{-1}$. Thus, $\mathbf{M}$ and $\mathbf{Z}_{\text{rad}}\, \mathbf{Z}_{\text{pow}}{}^{-1}$ have the same eigenvalues, counting multiplicity [13, § 1.3]. Consequently $\lambda_1,..., \lambda_m$ are the eigenvalues of $\mathbf{Z}_{\text{rad}}\, \mathbf{Z}_{\text{pow}}{}^{-1}$, counting multiplicity, which are real, these eigenvalues being labeled in ascending order.

In the case where $\mathbf{I}_0$ is known, a value of e can be computed, which lies in $[\lambda_1, \lambda_m]$. In the case where $\mathbf{I}_0$ is not known, $\mathbf{I}_0$ can be considered as a random complex vector. In this case, if we had suitable information on the statistics of $\mathbf{I}_0$, we could derive the expectation $< e >$ of e, which lies in $[\lambda_1, \lambda_m]$. Following a different approach, we note that, according to the Courant-Fischer "min-max theorem" [13, § 4.2] each eigenvalue of $\mathbf{M}$ is a stationary value of e. We can define an "average" value of e, denoted by e_{MP}, as the average of these eigenvalues. Since

$$\sum_{i=1}^{m} \lambda_i = \operatorname{tr} \mathbf{M} = \operatorname{tr}\left(\mathbf{Z}_{\text{rad}}\, \mathbf{Z}_{\text{pow}}^{-1} \right) \tag{41}$$

our average value e_{MP} is given by

$$e_{MP} = \frac{1}{n} \operatorname{tr}\left(\mathbf{Z}_{\text{rad}}\, \mathbf{Z}_{\text{pow}}^{-1} \right) \tag{42}$$

We note that e_{MP} lies in $[\lambda_1, \lambda_m]$, and that e_{MP} can be regarded as an expectation of e for an assumed statistics of $\mathbf{I}_0$.

V. Conclusion

We have studied the matrix of the beam cosines of the radiated power of an MAA and the matrix of the beam cosines of the delivered power of the MAA. These matrices are complex and they need not be equal. However, we have explained why, in some special cases, they can be real and equal.

We have defined the radiation efficiency of an MAA, in a manner that is consistent with the definition used for a single antenna. The radiation efficiency depends on the excitation. However, a minimum value, a maximum value and an average value of the radiation efficiency can be computed.

References

[1] N. Murtaza, M. Hein and E. Zameshaeva, "Reconfigurable decoupling and matching network for a cognitive antenna", *Proc. 41st European Microwave Conf. (EuMC)*, pp. 874-877, Oct. 2011.

[2] X. Tang, K. Mouthaan and J.C. Coetzee, "Tunable decoupling and matching network for diversity enhancement of closely spaced antennas", *IEEE Antennas and Wireless Propagat. Letters*, vol. 11, pp. 268-271, 2012.

[3] A. Krewski and W.L. Schroeder, "Electrically tunable mode decomposition network for 2-port MIMO Antennas", *Proc. of the 2013 Loughborough Antennas and Propagation Conf. (LAPC)*, pp. 553-558, Nov. 2013.

[4] F. Broydé and E. Clavelier, "Some Properties of Multiple-Antenna-Port and Multiple-User-Port Antenna Tuners", *IEEE Trans. on Circuits and Systems — I: Regular Papers*, Vol. 62, No. 2, pp. 423-432, Feb. 2015.

[5] F. Broydé and E. Clavelier, "Two Multiple-Antenna-Port and Multiple-User-Port Antenna Tuners", *Proc. 9th European Conference on Antenna and Propagation, EuCAP 2015*, April 2015.

[6] F. Broydé and E. Clavelier, "A Tuning Computation Technique for a Multiple-Antenna-Port and Multiple-User-Port Antenna Tuner", *International Journal of Antennas and Propagation*, vol. 2016, Nov. 2016.

[7] S. Lang, *Undergraduate analysis*, Springer-Verlag, 1983.

[8] R.E. Collin, *Antennas and Radiowave propagation*, International Edition, McGraw-Hill, 1985.

[9] K. Wang, L. Li and T.F. Eibert, "Estimation of Signal Correlation of Lossy Compact Monopole Arrays With Decoupling Networks", *IEEE Trans. Antennas Propagat.*, vol. 63, No. 1, pp. 357-363, January 2015.

[10] S. Blanch, J. Romeu and I. Corbella, "Exact representation of antenna system diversity performance from input parameter description", *Electronics Letters*, vol. 39, No. 9, pp. 705-707, May 2003.

[11] K. Fujimoto, *Mobile Antenna System Handbook*, Third Edition, Artech House, 2008.

[12] E. Ramis, C. Deschamps and J. Odoux, *Cours de mathématiques spéciales — 2 — Algèbre et applications à la géométrie*, Masson, 1979.

[13] R.A. Horn, C.R. Johnson, *Matrix analysis*, Cambridge University Press, 1985.

[14] S. Stein, "On Cross Coupling in Multiple-Beam Antennas", *IRE Trans. Antennas Propagat.*, vol. 10, No. 5, pp. 548-557, Sept. 1962.

[15] M. Hamermesh, *Group Theory and its Application to Physical Problems*, Dover, 1962.

[16] R. Vaughan and J.B. Andersen, "Antenna Diversity in Mobile Communications", *IEEE Trans. Veh. Technol.*, vol. 36, No. 4, pp. 149-172, Nov. 1987.

[17] M.A. Moharram and A.A. Kishk, "MIMO Antennas Efficiency Measurement Using Wheeler Caps", *IEEE Trans. Antennas Propagat.*, vol. 64, No. 3, pp. 1115-1120, March 2016.

[18] IEEE Std 145-2013, IEEE Standard for Definitions of Terms for Antennas, 2013.